

FINAL REPORT

High Temperature Ultrasonic Transducers:  
Material Selection and Testing

SUPERVISOR:

Dr. Yoseph BAR-COHEN  
NDEAA Lab - JPL  
**Caltech**

STUDENT:

Alessandro BRUNO  
Scuola Superiore Sant'Anna, Italy

September 28, 2012

# Contents

<b>1</b>	<b>Introduction and Testbed</b>	<b>3</b>
<b>2</b>	<b>Measuring devices and interfaces</b>	<b>6</b>
2.1	Environmental chambers . . . . .	6
2.2	Echo-pulse test equipment . . . . .	7
2.3	Impedance Scanning test equipment . . . . .	10
2.4	Software . . . . .	10
2.5	Experimental setup . . . . .	19
<b>3</b>	<b>Bibliographic Survey and Commercial Examples</b>	<b>23</b>
3.1	Commercial Examples examined at NDEAA Lab . . . . .	23
3.2	Other Commercial Examples . . . . .	24
3.3	Bibliographic Survey . . . . .	26
<b>4</b>	<b>Piezoelectric Material Selection</b>	<b>32</b>
4.1	Curie Temperature . . . . .	32
4.2	Qualitative Tests . . . . .	33
4.3	Test of PZT5-851 piezoceramics . . . . .	36
4.3.1	In-Temperature Measurements . . . . .	36
4.3.2	Quantitative Results . . . . .	36
4.4	Test of TapeCast PZT5A Piezoceramics . . . . .	40
<b>5</b>	<b>Fabrication Technologies and Materials</b>	<b>46</b>
5.1	Electrical Connection . . . . .	46
5.1.1	Electrodes . . . . .	46
5.1.2	Soldering . . . . .	46
5.1.3	Silver Painting and Conductive Polymers . . . . .	47
5.2	Polymer Molding . . . . .	49
<b>6</b>	<b>In-House Built Prototypes</b>	<b>51</b>
6.1	Early prototypes . . . . .	51
6.2	Prototypes . . . . .	53
6.2.1	Polymeric multilayer transducer . . . . .	53
6.2.2	No matching layer / bulk brass backing . . . . .	54

6.2.3	Thin copper-copper assembly . . . . .	55
<b>7</b>	<b>Summary</b>	<b>59</b>
7.1	Conclusions . . . . .	59
7.2	Issues and open problems with proposed solutions . . . . .	60

# Chapter 1

## Introduction and Testbed

**Introduction** The New York City steam system is a district heating system which takes steam produced by steam generating stations and carries it under the streets of Manhattan to heat or supply power to high rise buildings and businesses. Some New York businesses and facilities also use the steam for cleaning, climate control and disinfection. Consolidated Edison, Inc. (ConEd) operates this steam system, that with its 105 miles of mains and service pipes is the largest in the United States. In Manhattan, 1800 customers are served by this system. Table 1.1 shows steam vapor being vented on a street of Manhattan because of a leak in the system or produced by cooler water contacting the outside of a steam pipe.

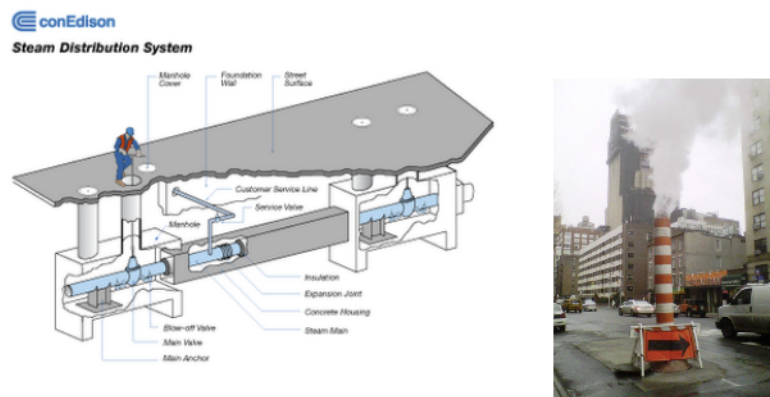


Table 1.1: A schematic of a manhole to access a steam pipe, steam being vented.

In order to prevent the formation of liquid water that could slow the steam flow, the pipes have to be periodically inspected. The level of condensed water could be monitored for long times using ultrasounds. The objective of NDEAA lab was to develop a fixture (strap) and a transducer capable of continuous operation at the temperature of 250°C, that is the requirement set by ConEd. The task of my

two-months internship was to test different materials to be used to build an high temperature transducer, to develop some prototypes and to test their performance, to asses the reliability of a commercial product rated for such a temperature, as well as to collaborate in developing the signal processing code to measure the condensed water level.

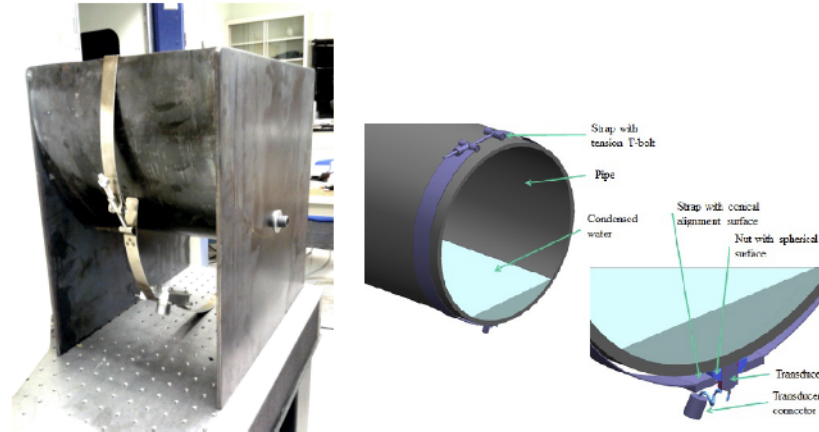


Table 1.2: The half-pipe section testbed with an aluminum prototype of the fixture, schematics of the strap.

**Testbeds** Table 1.2 shows the strap used to test the different transducers on a steel half-pipe testbed. The thickness of the pipe is 1 cm, while the external diameter is 40 cm. Being the environmental chamber not pressurized, the test fluid used was a lubrication silicon oil with a long term stability up to 250°C(Diphenyl-Dimethyl Silicone 400, Clearco Products).

Some problems about that fluid still have to be addressed: the speed of sound on this test fluid has been measured only at room temperature while, as explained in [2] and in many basic ultrasound textbooks, the bulk modulus, and consequently the speed of sound, decrease with the temperature. When will be possible to measure the oil level with a millimeter precision, will be possible to calculate the speed of sound at different temperatures, taking into account the large expansion coefficient of the oil and the geometry of the half pipe. Another issue with that particular fluid is the attenuation coefficient. As described in [3], the attenuation coefficient of silicone oil is larger than the water one of many orders of magnitude. Furthermore, as reported in [2], the amount of absorbed ultrasound energy in viscous media could decrease significantly with the temperature, making difficult to relate a change of the echo energy to the performance of the transducer only. For the previous reasons, many tests have been performed on a simple aluminum block.

# Bibliography

- [1] *Consolidated Edison website <http://www.coned.com/steam/>*
- [2] *Propagation of Ultrasonic Waves in Viscous Fluids, Oudina Assia and Djelouah Hakim, Faculty of Physics, University of Sciences and Technology Houari Boumedienne.*
- [3] *Attenuation of Ultrasound in Silicone-Oil-in-Water Emulsions, A. Schroder d E. Raphael, EUROPHYSICS LETTERS 1992*

## Chapter 2

# Measuring devices and interfaces

### 2.1 Environmental chambers

The environmental chamber originally available in the lab is the SPX Blue M Electric shown in the left picture of Table 2.1. This furnace could be programmed to target different temperatures or to vary the temperature at a given rate. The temperature sensor that drives the controller of this furnace measures the internal walls temperature. The air temperature, during an heating process carried out at the default rate, is about 15 °C less than the temperature of the walls. For this reason, a more accurate measurement of the specimen under test is usually taken with the Type K thermocouple, whose voltage could be read with a National Instrument USB-TC01 measuring device, shown in Figure 2.2. This environmental chamber is large enough to contain the half-pipe section testbed, but because of its dimensions, when heated over 250 °C takes more than 2 hours to cool down to less than 100 °C, that is a comfortable temperature to open the front door and possibly manipulate objects inside the chamber using thermal oven gloves.

In order to run high temperature tests in a more flexible way, the smaller environmental chamber EC10 (right picture in Table 2.1) manufactured by Sun Electronic Systems has been set up. This chamber is capable of using liquid nitrogen or  $CO_2$  as a coolant, but it's possible to operate it also with a normal air cooling. The EC10 features excellent communication capabilities since it's equipped with an analog port, a GPIB (IEEE488) port and a parallel port (RS-232 with a minimal "3-wire" connection, as explained in [2]). This chamber is provided with a fail safe switch that shuts down the whole system if a certain temperature is reached. During the first run, the fail safe switch triggered at 205 °C and was then necessary to raise the maximum allowed temperature to 275 °C following the instruction of the manual [2]. The EC10 is equipped with a temperature sensor that measures the wall temperature and with its own deployable thermocouple. A lateral port and a special foam plug allow bringing cables and connectors inside the



Table 2.1: The Blue M Electric SPX and the Sun Electronics EC10 environmental chambers.



Table 2.2: A termocouple attached to a National Instrument USB-TC01 measuring device

chamber without thermal loss. The EC10 chamber was always used by manually programming the PID controller, but thanks to its features, in the future it could also be controlled remotely using a PC.

## 2.2 Echo-pulse test equipment

In order to drive generic piezoelectric actuators and measure the voltage and the current, NDEAA lab is equipped with systems composed of waveform generators, amplifiers and an oscilloscopes. The specific version of this system designed to drive an ultrasonic probe is composed of an analog pulser/amplifier PANAMETRIX 5052PR and the digital oscilloscope TEKTRONIX TDS2024B.

**Pulser/Amplifier** The PANAMETRIX 5052PR is a device specifically designed for Nondestructive Testing. The general working principles of a Pulser/Amplifier



Table 2.3: PANAMETRIX 5052PR Pulser/Amplifier

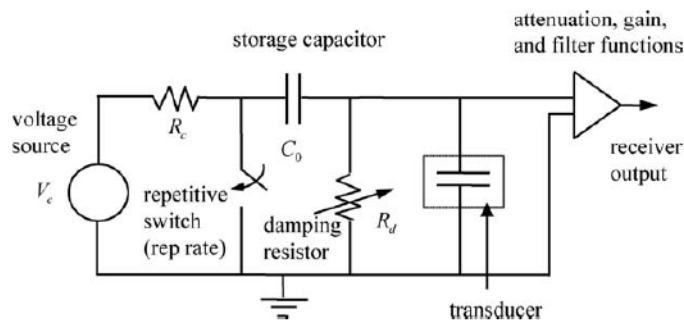


Table 2.4: Extremely simplified schematics of a Pulser/Amplifier.

device are described in [1]. Such a device could be effectively divided in a Pulser part and an Amplifier part and also the position of the controls on the front panel (Table 2.3) highlights that distinction. Figure 2.4 shows an extremely simplified schematics of the device.

The controls REP RATE, ENERGY and DAMPING are relative to the Pulser part and determine, respectively, the frequencies of the spikes, the energy stored in the capacitor (that is proportional to the capacitor capacitance) and the resistance of the damping resistor. Since the capacitance-resistance-transducer grid could be modeled as an RC resonating circuit, the characteristic damping time is altered by changing the value of the damping resistance, that is, by producing an high-pass filter. Further filtering is made by the Amplifier part that, in this model, is supposed to have an high input resistance and doesn't affect in any way the Pulser part.

In [1] is also described the method to calculate the value of the equivalent circuitual components of the Pulser, in order to model properly the interaction with any different transducer. Since the impedance of the piezoelectric transducers vary with the temperature, such a modeling of the interaction between the Pulser and the transducer could be used in the future to vary the circuitual parameters

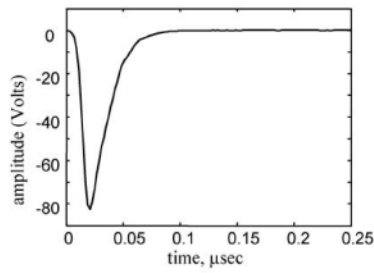


Table 2.5: Waveform of the spike produced by the Pulser/Receiver when attached to an high impedance.

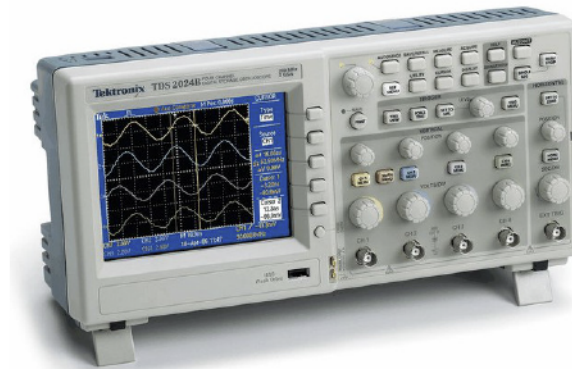


Table 2.6: TEKTRONIX TDS2024B oscilloscope.

accordingly to the temperature in order to obtain the best echo signal possible, in terms of amplitude and noise damping.

**Oscilloscope** The TEKTRONIX TDS2024B (Table 2.6) is a general purpose oscilloscope capable of a sampling rate of 2 GS/s and a usable bandwidth of about 200 MHz. After being triggered, the oscilloscope is capable of recording 2500 data points. Limited data could be stored in an internal memory or in a memory stick. The oscilloscope is connected to a trigger source, to the signal source and to a PC via an USB port. In order to establish a GPIB-like serial communication and store data directly on the PC, it's necessary to install a USBTMC (USB Test and Measurement Class) open source driver, that is a common requirement for USB measuring devices. On Linux and Windows systems, the communication is then trough a virtual GPIB interface. Other proprietary drivers are necessary to control the Oscilloscope using LabView.

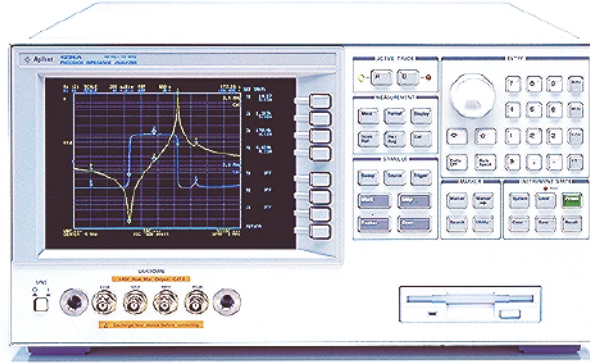


Table 2.7: Agilent HP4294A impedance analyzer.

## 2.3 Impedance Scanning test equipment

The Agilent HP4294A (Table 2.7) is a precision industrial impedance analyzer. This instrument allows to measure the impedance (complex impedance or equivalent circuits parameters) of a piezoelectric device at different frequencies. A limited amount of impedance scannings could be stored in the internal memory or in a floppy drive. It's also possible to write BASIC-like program to be executed from the internal memory. The device have to be calibrated to compensate the impedance of any adaptors/cable used instead of the standard grippers following the instruction on its manual [3]. This device is featured with a GPIB (IEEE488) port, a 24 and 8 bit I/O ports and an Ethernet port. As explained in the programming manual [4], the Ethernet connection allows for Telnet serial communication, standard FTP file exchange and a peculiar kind of sockets communication. The GPIB and the Telnet interface share the same programming language. The communication capabilities of this impedance scanner are ideal to build highly automated experimental setups.

## 2.4 Software

**Controlling the Oscilloscope** The original interface available in the lab to control the Tektronix Oscilloscope was written in LabView. This program compute the autocorrelation of the signal in order to identify the echoes, as well as the time of flight and the fluid depth. The program was updated in collaboration with

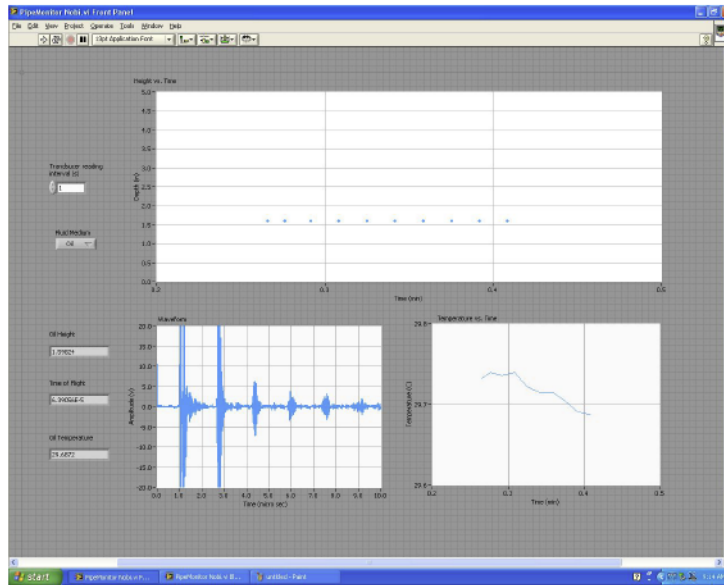


Table 2.8: User interface of the LabView program.

other researcher to allow continuous storing of the retrieved waveforms. The 2500 8-bit precision data points are acquired using the Binary format in approximately 210 microseconds. The bottleneck that limits the speed of the LabView interface, making it able to retrieve less than a single waveform per second, seems to be due to the poor performance of the program itself, or to the burden of handling a complex graphical interface ("Front panel", shown in Table 2.8). A reduction of the refresh rate of the user interface will improve the performance, as well as the implementation of an algorithm that suspends the data visualization when a higher sampling rate (waveforms per second) is required, for example when major changes in the echos are detected.

The main issues encountered working with LabView were related to the difficulties to handle an unstructured and insufficiently commented program. The block diagram of the program after some updates is shown in Tables 2.9 and 2.10.

In order to demonstrate that a traditional programming alternative to LabView is feasible, a Python script was developed. Python is a general-purpose, interpreted high-level programming language. Its interpreter under Windows and UNIX systems is free and open-source. Because of this, implementation of Python and its expansion packages could be performed on any machine without any license. Because of the complex JPL license deployment system, obtaining the proper license to run proprietary software could become a major concern on non-standard computers, such as the Embedded PC's designed for field testing. Python is very popular in the particle physics community and it's regarded to be as reliable as proprietary programs. The following Python script performs most of the tasks of

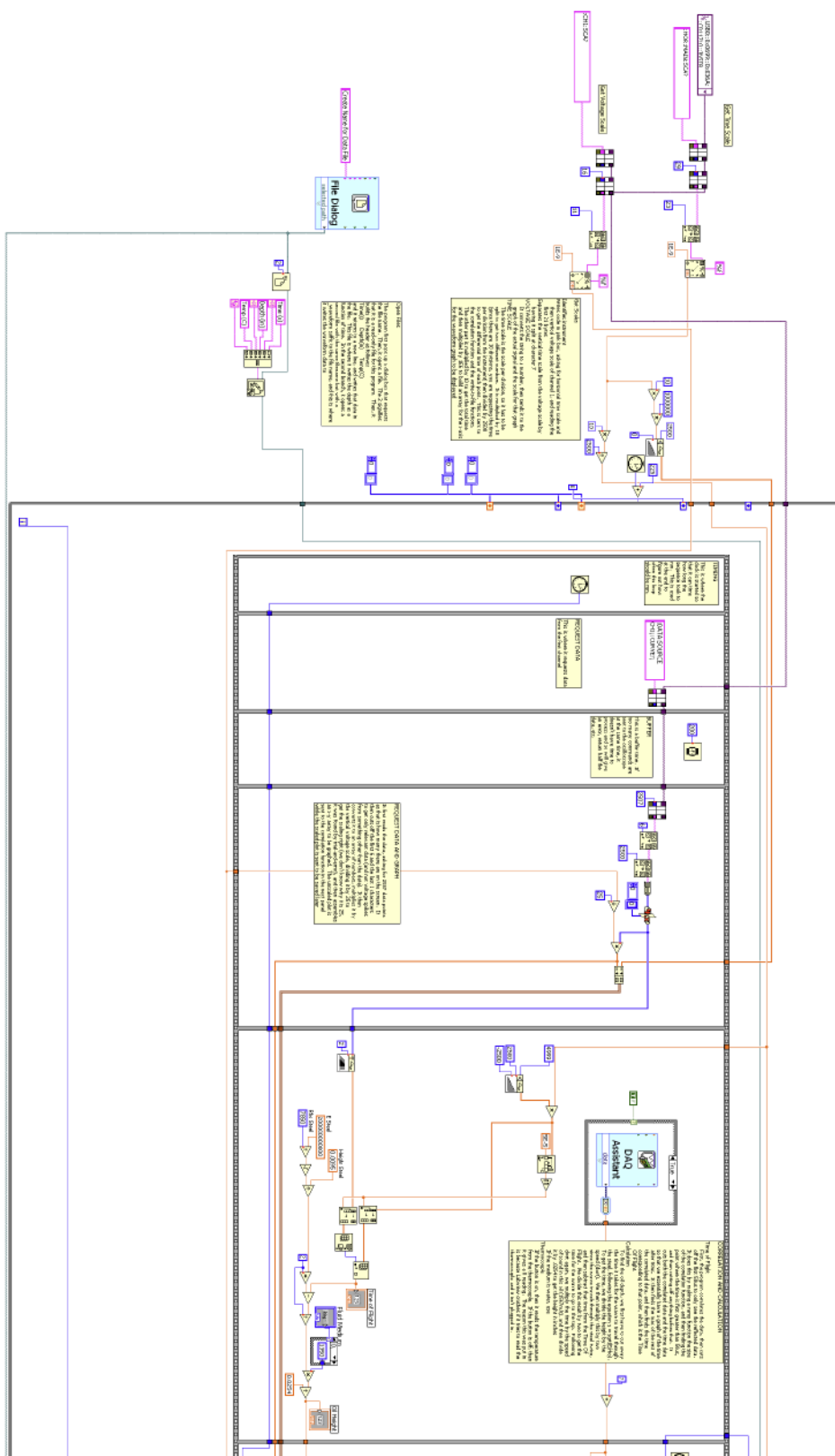


Table 2.9: Block Diagram of the LabView interface (part 1).

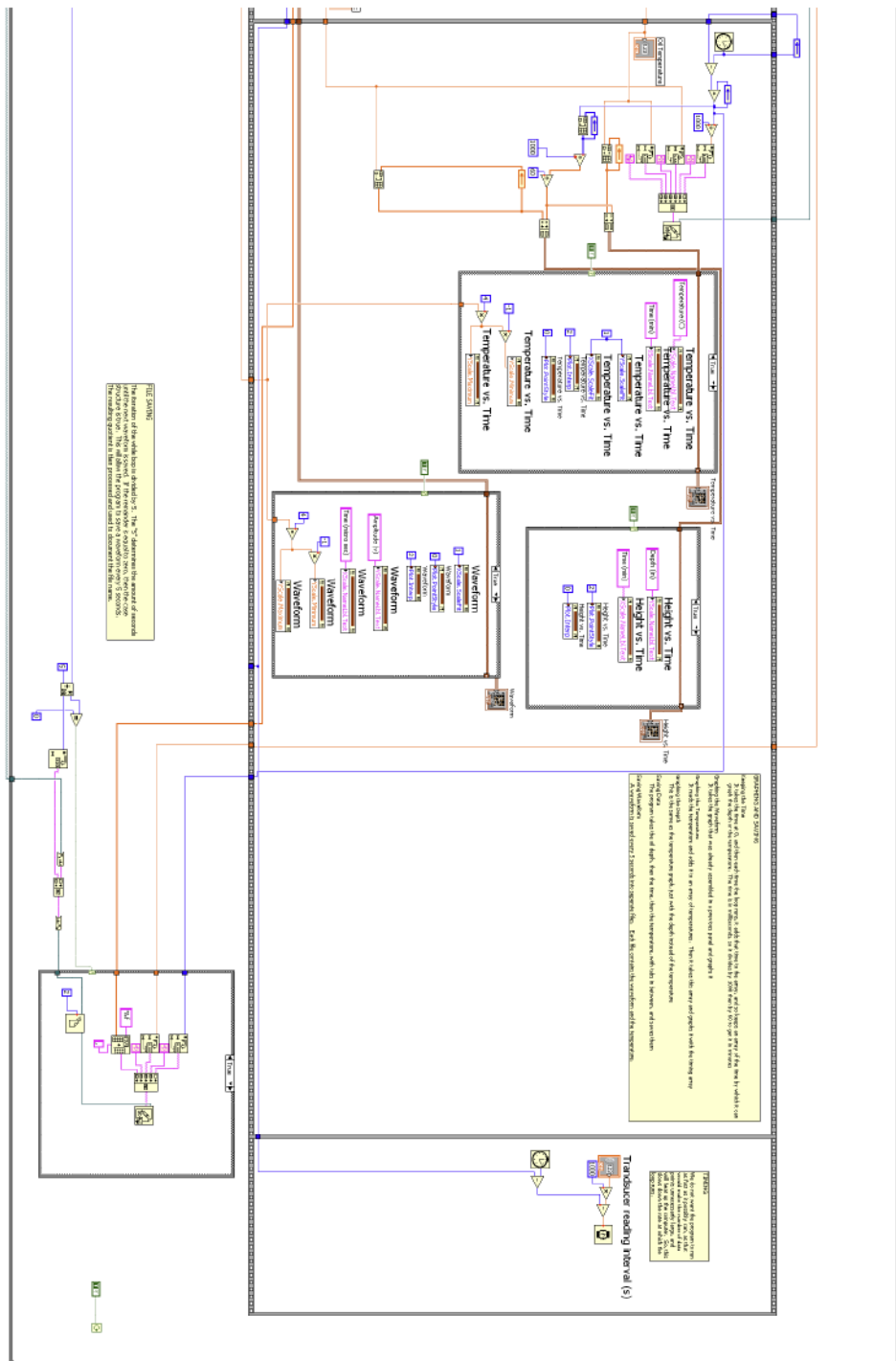


Table 2.10: Block Diagram of the LabView interface (part 2).

the LabView program, that is, retrieves the waveform data, plot and store it on a file. This script could be easily rearranged in a class to be implemented in a larger program capable of performing the signal processing computation. The non capital letters in the GPIB commands are optional.

```
# Python GPIB interface for Tektronix 2024B
# NDEAA Lab - Jet propulsion Laboratory
# Version 1.0
# Alessandro Bruno - al.bruno@sssup.it

import visa
import time
import StringIO
import csv
import numbers
import numpy
from struct import unpack
import scipy
import matplotlib.pyplot

# Print the title of the program
print "Signal Processing for Ultrasonic Edge Detection"
print "NDEAA Lab - Jet Propulsion Laboratory"

# Define a device object
oscilloscope = visa.instrument("USB0::0x138A::0x0005::3911ac4ce700::RAW")

# Diagnostics: ask the device for its name
print oscilloscope.ask("*IDN?")

# Set the data source
oscilloscope.write("DATA:SOUrce CH1")

# Set the data encoding to the ASCII format
oscilloscope.write("DATA:ENCdg RIB")

# Set the byte representation mode
# oscilloscope.write("WFMO:BYTE_NR 2")

# Set the data width (as in Factory settings)
oscilloscope.write("DATA:WIDth 1")

# Set the position of the first sample, in XUNITS relative to the trigger signal.
oscilloscope.write("WFMPre:XZEro 0")

# Read the position of the first sample in XUNITS
```

```

XZEROstring = oscilloscope.ask("WFMPre:XZero?")
XZEROstring = XZEROstring.split(' ')[1]
XZERO = float(XZEROstring)

# Read the offset in YUNITs
YZEROstring = oscilloscope.ask("WFMPre:YZERO?")
YZEROstring = YZEROstring.split(' ')[1]
YZERO = float(YZEROstring)

# Read the offset in YUNITs
YOFFstring = oscilloscope.ask("WFMPre:YOFF?")
YOFFstring = YOFFstring.split(' ')[1]
YOFF = float(YOFFstring)

# Read the Y multiplier
YMULTstring = oscilloscope.ask("WFMPre:YMult?")
YMULTstring = YMULTstring.split(' ')[1]
YMULT = float(YMULTstring)

# Read the X increment between datapoints
XINCRstring = oscilloscope.ask("WFMPre:XINcr?")
XINCRstring = XINCRstring.split(' ')[1]
XINCR = float(XINCRstring)

# Read data points from the oscilloscope.
stringdatapoints = oscilloscope.ask("CURVe?")

# Debug only: print the preamble
print oscilloscope.ask("WFMPre?")

# Read data points from the oscilloscope.
stringdatapoints = oscilloscope.ask("CURVe?")

# Process the binary data
rawdapoints = numpy.frombuffer(stringdatapoints, dtype = numpy.dtype('int16').newbyteorder('S'))

print rawdatapoints

for i in range(0,len(rawdatapoints)):
    print rawdatapoints[i]

# Debug only: test the transfer speed
startingtime = time.clock()
for y in range(0,10):
    stringdatapoints2 = oscilloscope.ask("CURVe?")

```

```

elapsedtime = time.clock() - startingtime
print "Total time elapsed for 10 data transfers: ", elapsedtime, " seconds."

# Debug only: show constants
print "xzero is ", XZERO
print "yoff is ", YOFF
print "xincr is ", XINCR
print "ymult is ", YMULT
print "yzero is ", YZERO

# Calculate data points
datapoints = YMULT*(YOFF+rawdatapoints) +YZERO

# Debug only:
for i in range(0,len(datapoints)):
    print datapoints[i]

timepoints=numpy.arange(0,XINCR*len(datapoints),XINCR)

# Plot the waveform
matplotlib.pyplot.plot(timepoints,datapoints)
matplotlib.pyplot.show()

```

**Controlling the Impedance Scanner** A Matlab program was developed to communicate with the Impedance Scanner using the Telnet protocol. The program create a timer object that periodically launch a script to retrieve the current impedance spectrum. The following is the code of its main M-file:

```

% Matlab interface for Agilent HP4294A
% NDEAA Lab - Jet propulsion Laboratory
% Version 1.0
% Alessandro Bruno - al.bruno@sssup.it

% Main program

%Constants settings
time_delay = 5*60
%Start and End Frequencies (read them on the device)
start_freq = 2e6
end_freq = 3e6
filename = 'impedance_scan_'

%Reset counter

```

```

counter = 0;

%Create a timer object
scanner = timer

%Set the execution mode, the function to be executed,
%and the time delay between the start of each execution
set(scanner,'executionMode', 'fixedRate')
set(scanner,'TimerFcn','read_data')
set(scanner,'period',time_delay)
get(scanner)

start(scanner)

```

The script relies on the open source Telnet client GNU Netcat. The answers to any request to the Impedance Analyzer is streamed on the operating system standard output and is read by the Matlab script.

```

% Script read_data.m

%Update the counter
counter = counter + 1;

%Display the acquisition starting message
counter_string = num2str(counter)
message = strcat('Acquisition ',counter_string, ' in progress.')
display(message)

%Build the command string
input_file = strcat('command.txt');
output_file = strcat(filename,counter_string,'.txt');
command1 = strcat(current_directory,'nc 192.168.1.3 23 -v -w 7 < ');
command = strcat(command1,input_file, ' > ', output_file)

%Debug only
[status,result] = system('dir','-echo');

[status,result] = system(command,'-echo');

```

The list of the GPIB commands to sent is provided to the Netcat program trough a command.txt file, that in this minimal example read as follows:

```
*IDN?
```

:OUTPDATA?

**Data post processing** All the programs previously described save raw data as text files. In order to analyze those data, some Matlab parsing scripts has been developed. The following loads all the waveforms recorded with the LabView program in a single Matlab matrix:

```
% Example of parsing program for LabView output
% The file name is defined in the filename string variable
% example: filename = 'test'

filename = 0

while true

filename_string = num2str(filename);
completfilename = strcat(filename ,filename_string);

% Read each waveform file , store them in a matrix.

% Tries to open the file, if it doesn't succeed, it will exit from the
% while loop.
try
    fileID = fopen(completfilename)
catch
    message = strcat('Acquired ' ,filename_string, ' files.')
    display(message)
    break
end

% Read the files
A = fscanf(fileID, '%s\t%s\t%s')

% Split the string
parts1 = regexp(A, ',', 'split');
part2 = regexp(parts1(1), '.', 'split');

% Read the time
timestring = part2(1);

% Count in how many chunks A has been splitted
nel = size(parts1);
nel = nel(2);
```

```

% Extract the interesting chunk
datapointsstring = parts1(2:nel);

% Convert to double
datapoints = str2double(datapointsstring);

% Stores datapoints in a matrix
waves(filenumber+1,:) = datapoints(:);

message = strcat('File ',filenumber_string, ' acquired.')
    display(message)

%Increase the counter
filenumber = filenumber +1;

end

```

A similar script has been written to read the impedance scannings retrieved with the Matlab-GNU Netcat program. All the previous scripts could be rewritten in order to save data in a more consistent format, such as CSV (comma separated ASCII file) or binary.

## 2.5 Experimental setup

The wiring for the echo-pulse experiments inside the Environmental Chamber are summarized in Table 2.11. The Pulser/Amplifier triggers the oscilloscope through the TRG channel, while sending pulses to the ultrasonic transducer, that is connected with an high temperature coaxial cable. The signal is transmitted to the oscilloscope, that communicates with the computer running the LabView or the Python program via an USB connection as previously described. The computer stores also the temperature data using a proprietary National Instrument logging program or a subroutine of the previously described LabView program.

The wiring for the impedance scanning experiments inside the Environmental Chamber is shown in Table 2.12. This time, the computer is connected with an Ethernet cable and is running the Matlab-Netcat program already described.

In the future will be possible to carry out very extended or complex high temperature tests controlling the Environmental Chamber through the parallel port. Using TCP/IP socket communication, or a simple SMTP mail server, the status of the system could be easily monitored from remote, allowing overnight testing. This proposed setting is shown in the Table 2.13.

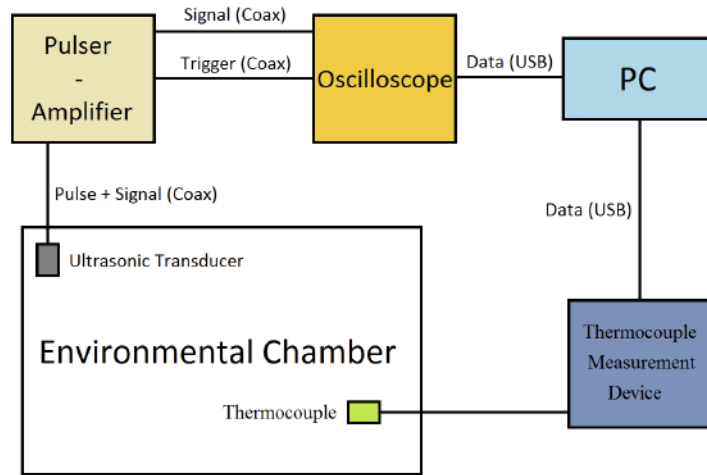


Table 2.11: Wiring for the echo-pulse experiments.

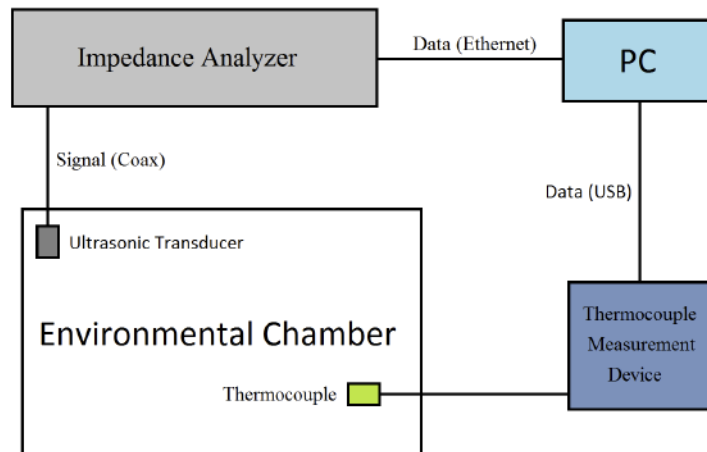


Table 2.12: Wiring for the impedance scanning experiments.

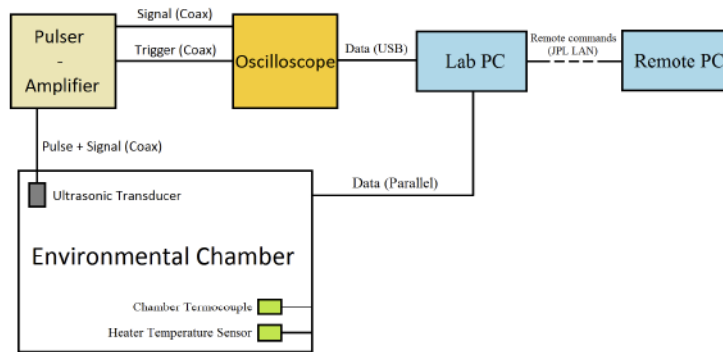


Table 2.13: Proposed settings for very extended automatic testing.

# Bibliography

- [1] *Ultrasonic Nondestructive Evaluation Systems, Models and Measurements*, Schmerr L., Song J., Chapter 2 (Springer 2007)
- [2] *Environmental Chamber EC10 User Manual*, Sun Electronics Systems
- [3] *Agilent 4294A Precision Impedance Analyzer Operation Manual, Fourth Edition*
- [4] *Agilent 4294A Precision Impedance Analyzer Programming Manual, Eighth Edition*
- [5] *TDS1000 and TDS2000-Series Digital Storage Oscilloscope*, Tektronix
- [6] *TDS200, TDS1000/TDS2000, TDS1000B/TDS2000B, and TPS2000 Series Digital Oscilloscopes Programming Manual*, Tektronix
- [7] *Python online documentation* <http://www.python.org/doc/>

## Chapter 3

# Bibliographic Survey and Commercial Examples

### 3.1 Commercial Examples examined at NDEAA Lab

NDEAA Lab examined in the past two different kind of high temperature ultrasonic transducers. The first kind of design, shown in Figure 3.1, is composed of a polymeric casing surrounding the piezoelectric disk and a tungsten-polymer backing to absorb waves directed toward the rear part of the transducer. The matching layer is polymeric as well, and the flat wire (less than 0.5 mm wide and approximately 0.1 thick) are soldered to the electrode. As it's possible to see in microphotographs of a dismantled model (Table 3.1), the soldering material layer is extremely thin. This observation suggest that the electrodes weren't soldered using a traditional techniques. Transducer of this kind are manufactured by Sigma Transducers, Inc, but all the models examined at NDEAA Lab had some structural integrity problem when exposed to 250 °C.

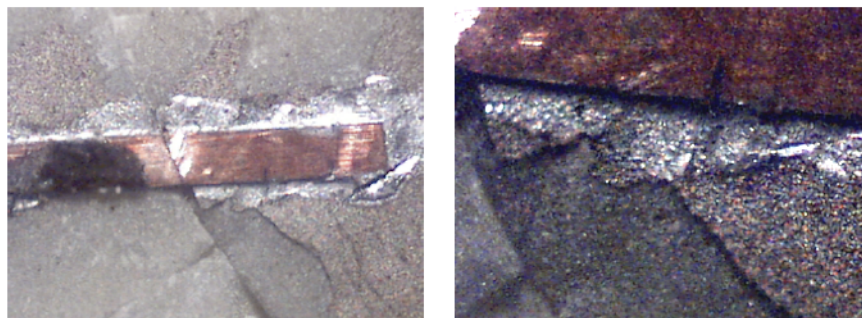


Table 3.1: Flat wire soldered on front electrode, transducer manufactured by Sigma, Inc. Optical Microscope 60X 200X

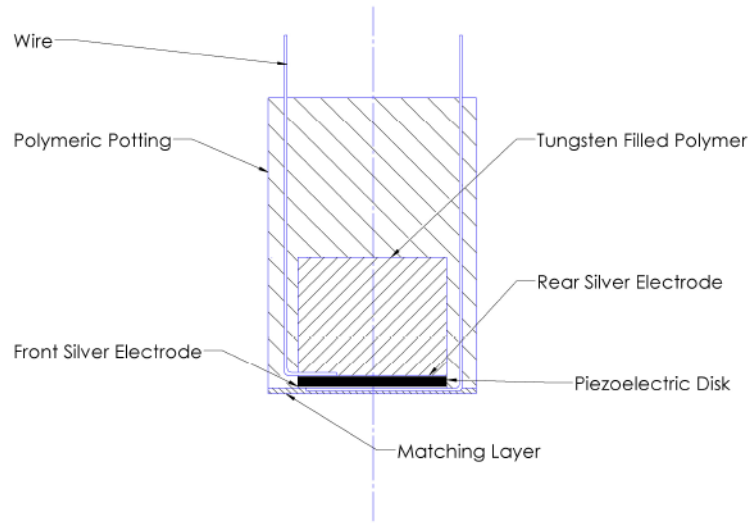


Figure 3.1: General schematics of a transducer with a polymeric structure.

A different design is shown in Table 3.2. In this design, there is no backing layer, while the matching layer is metallic. The whole case act as a ground electrode and the signal wire is connected to the rear electrode of the transducer. In an early version of this model, manufactured by NDT Transducers, the metallic matching layer detached from the front part of the case. An updated version of the same model is currently under test at NDEAA Lab. Preliminary results are summarized in the next chapters.

## 3.2 Other Commercial Examples

A first literature search was made to gather some knowledge about the composition of transducers backing and the general transducer building process.

Commercial examples of high temperature ultrasonic probes are the two General Electric transducers shown in Table 3.2. Those transducers (models 66593 SEB 4 KV and 67471 B 4 GVN) are capable of continuous operation on surfaces at 250 °C, but the manufacturing company doesn't provided any information about the allowed environmental temperature. Other companies claiming to be able to produce transducers working continuously at 250 °C are Applus RTD and Gilardoni (see [Applus Catalog] and [Gilardoni Catalog]). No information is provided about the materials and the manufacturing process. As reported by [Correia],

*Generally is very difficult to find the appropriate technical informa-*

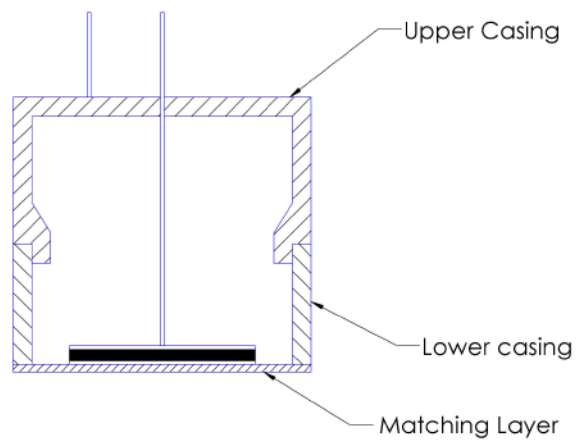


Figure 3.2: General schematics of a transducer with an aluminum matching layer and no backing.

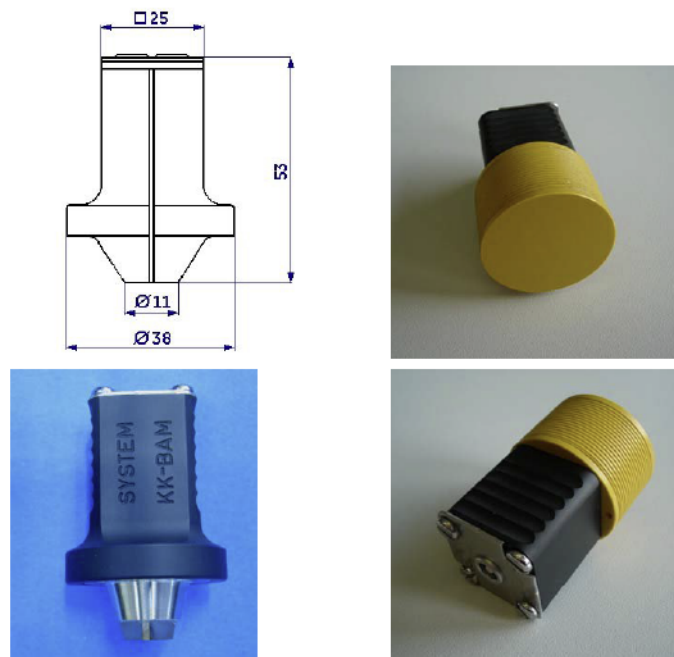


Table 3.2: General Electric 66593 SEB 4 KV and 67471 B 4 GVN ultrasonic transducers.

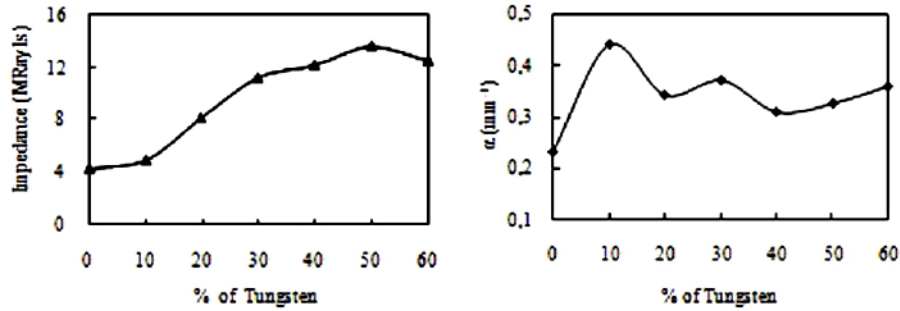


Figure 3.3: From [Correia]. Acoustic impedance and absorption coefficient of Bakelite-tungsten composites as functions of volume percentage of tungsten.

*tion to develop specific ultrasonic transducers because it is part of the "know how" of commercial companies.*

### 3.3 Bibliographic Survey

**Bakelite-Tungsten composites** Some articles and patents characterizing composite backing materials suitable to low temperature usage were found. [Correia] and [Rubio] describe the production of composites of Bakelite (thermosetting phenol formaldehyde resin) and tungsten. Both Bakelite and tungsten were provided as powders, mixed and then cured in an hydraulic press. The size of the tungsten particles reported in [Correia] is 0.6 - 1  $\mu\text{m}$ . Acoustic impedance and attenuation coefficient for different volume fractions are shown in Figure 3.3. As noted by [Correia], the maximum attenuation lies near the 10% of volume of tungsten, while the acoustic impedance seems to be an increasing function of the tungsten concentration.

**Epoxy-Aluminum composites** As shown in [Ruangsawad], Epoxy-Aluminum (*Al*) composites are effective as backing materials for probes to be operated in air. As shown in Figure 3.4, the attenuation increase with the concentration of aluminum powder in the mixture.

**Epoxy-Tungsten and Epoxy-Alumina composites** An extended analysis of the acoustical proprieties of Epoxy-Tungsten and Epoxy-Alumina ( $\text{Al}_2\text{O}_3$ ) composites is described by [Wang]. The article shows a simple relation developed by A. J. Devaney and H. Levine to calculate the bulk modulus, the shear modulus and consequently the real part of the acoustic impedance of two-phase composites, given the hypothesis that the ultrasound waves are scattered multiple times by the particles of a component and that each of those particle is surrounded by the other component. The speed of longitudinal waves in a solid medium is

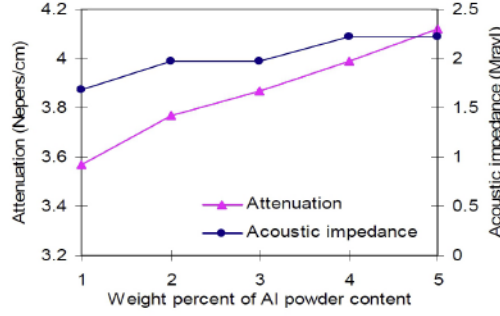


Figure 3.4: From [Ruangsawad]. Attenuation and acoustic impedance in Epoxy-Aluminum composites.

$$v = \sqrt{\frac{K + \frac{4}{3}G}{\rho}} \quad (3.1)$$

The density of the two-phase composite is the volume averaged density:

$$\rho = V_1\rho_1 + V_2\rho_2 \quad (3.2)$$

being  $V_1$  and  $V_2$  respectively the volume fraction of the matrix and of the particles. The equations referred to by [Wang] are the following:

$$K = K_1 + V_2 \frac{(3K + 4G)(K_2 - K_1)}{3K + 4G + 3(K_2 - K_1)} \quad (3.3)$$

$$G = G_1 + V_2 \frac{5(3K + 4G)G(G_2 - G_1)}{15K + 20G + 6(K + 2G)(G_2 - G_1)} \quad (3.4)$$

[Wang] doesn't report the solving method, but it's easy to solve that system of non linear equations numerically using Matlab. The article compares the predicted acoustic impedance of the epoxy-alumina and epoxy-tungsten composites with the experimental calculated ones. Results are shown in Figure 3.5 and 3.6, together with the acoustic attenuation measurement, for a test frequency of 30 MHz. It's possible to see that the acoustic impedance follows the model very well. As it's shown, the attenuation peak is between 7 and 9% volume fraction of particles filler.

As pointed out by [Grew], the attenuation coefficient depends on the size of the particles and it's only approximately linear with the frequency. As shown in Table 3.3, for a test frequency of 5 MHz and particle sizes between a fraction of micrometer and some micrometers, the attenuation increases strongly with the size of the particles. That article, together with the one from [Wang], is the best that was possible to get during this quick bibliographic survey.

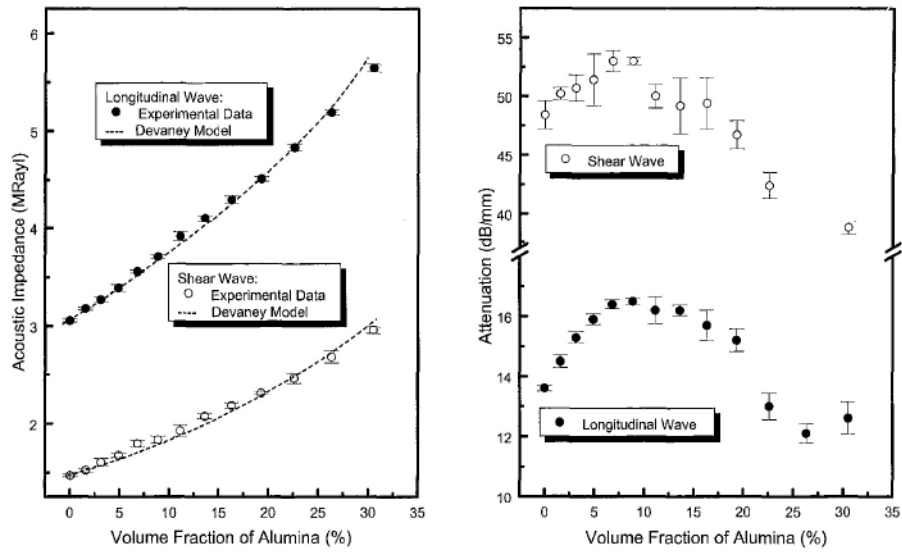


Figure 3.5: From [Wang]. Acoustic impedance and attenuation coefficient of epoxy-alumina composites. Test frequency: 30 MHz. Alumina particles diameter:  $3 \mu m$ .

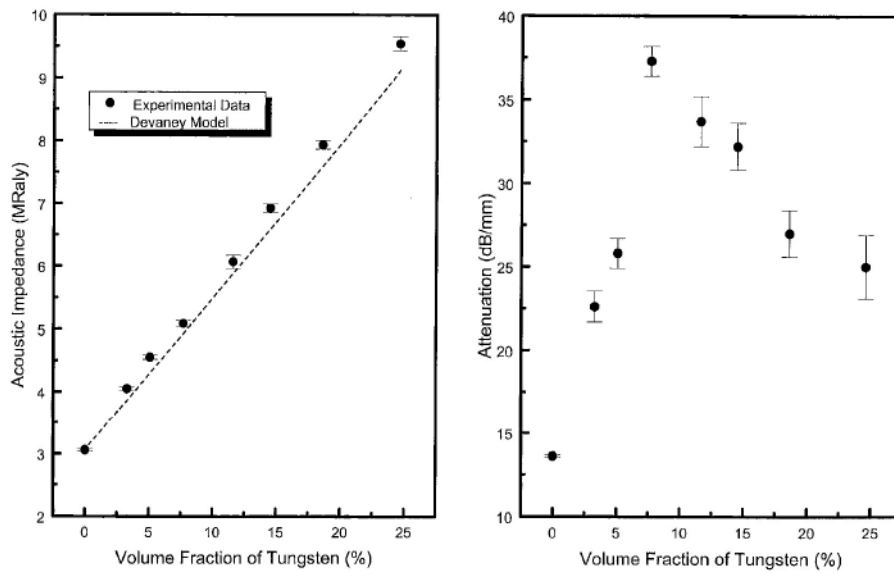


Figure 3.6: From [Wang]. Acoustic impedance and attenuation coefficient of epoxy-tungsten composites. Test frequency: 30 MHz. Tungsten particle size: less than  $5 \mu m$ .

**TABLE V**  
AVERAGE ACOUSTIC PROPERTIES OF ALUMINA/SPURR EPOXY COMPOSITES

Filler	Averages → Volume %	Measured Impedance (MRayl)	Calculated Impedance (MRayl)	Attenuation at 5 MHz (dB/cm)
Spurr Epoxy	100	2.5		19
Alumina	100	25		
Alumina				
0.3 μm	5.8 ± 0.6	3.3 ± 0.1	3.2	38 ± 6
1.0 μm	11.8 ± 0.8	4.0 ± 0.1	3.6	36 ± 4
3.0 μm	3.9 ± 0.3 10.4 ± 0.5	2.6 ± 0.0 3.1 ± 0.0	3.0 3.5	40 ± 6 25 ± 3
12.5 μm	4.4 ± 0.9 10.8 ± 0.4 40.6 ± 1.0	2.6 ± 0.1 3.1 ± 0.0 7.0 ± 0.2	3.1 3.5 5.4	3.5 ± 9 23 ± 2 22 ± 2

**TABLE III**  
AVERAGE ACOUSTIC PROPERTIES OF TUNGSTEN/SPURR EPOXY COMPOSITES

Filler	Averages → Volume %	Measured Impedance (MRayl)	Calculated Impedance (MRayl)	Attenuation at 5 MHz (dB/cm)
Spurr Epoxy	100	2.5		19
Tungsten	100	103		
Tungsten				
1 μm	10.6 ± 0.7 18.8 ± 0.6	4.9 ± 0.2 7.0 ± 0.2	5.0 6.5	45 ± 8 40 ± 5
3 μm	11.2 ± 1.2 19.6 ± 0.4 28.2 ± 0.6	5.1 ± 0.4 7.0 ± 0.2 9.7 ± 0.2	5.1 6.7 8.0	47 ± 8 39 ± 6
5 μm	9.9 ± 0.3 18.9 ± 0.7 31.9 ± 0.7	4.7 ± 0.2 6.7 ± 0.3 10.8 ± 0.4	4.9 6.5 8.7	69 ± 12 65 ± 8 42 ± 5
50 μm	36.4 ± 0.9 40.1 ± 0.9	12.8 ± 0.2 14.6 ± 0.7	9.4 10.2	246 ± 17 178 ± 17

Table 3.3: From [Grewe]. Attenuation and Acoustic impedance for epoxy-alumina and epoxy-tungsten composites. Test frequency: 5 MHz

	Backing Material	
	Tungsten-Epoxy	Tungsten-Cerium-Epoxy
Wave from pulse width	3 μsec	2 μsec
Wave form residual vibration	12 μsec	7 μsec

Figure 3.7: From [Ju-Zhen]. Comparison of residual wave duration in Tungsten-Epoxy and Tungsten-Cerium-Epoxy composites in same experimental conditions.

[Ju-Zhen] patented the fact that adding cerium oxide to the powder mixture improves the damping proprieties, as shown in Figure 3.7. The backing of the patented transducer is made of tungsten/cerium oxide filled epoxy. The powder added to the epoxy is claimed to be  $\frac{1}{8}$  of the total weight of the composite, while the cerium oxide is reported to be the 2% in weight of the powder.

**Very High Temperature** A list of proposed damping materials for very high-temperature applications was found in [Mrasek]. The article state that is possible to obtain good ultrasonic readings up to 700 °C using a lithium niobate ( $LiNbO_3$ ) transducer and a porous ceramic backing. That ceramics was manufactured by Kager Industrieprodukte, a German company specialized in high-temperature materials, and then coated with glass. The softened glass, together with the force generated by a spring, keeps the probe parts mechanically linked, as shown in Table 3.4 (right). The article describes also a simple experimental setting that allows to test different materials using a single piezoelectric disk. As shown in Table 3.4

(left), mechanical contact between components is assured using an external force. Provided that the components have sufficiently smooth surfaces, and eventually using a fluid couplant, a setting similar to Table 3.4 (left) could be assembled at NDEAA Lab to quickly evaluate a number of different materials. In order to have a pressure constant at different temperatures, force should be provided by means of gravity.

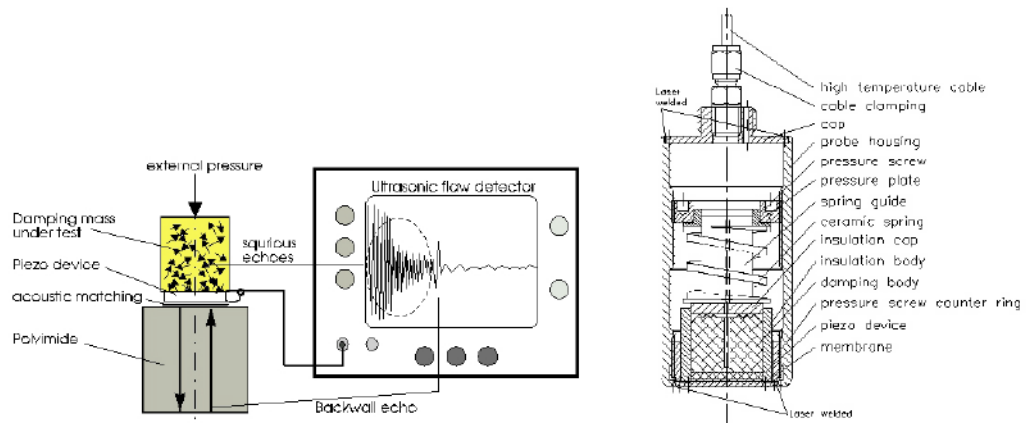


Table 3.4: From [Mrasek]. Left: experimental setting for backing material testing. Right: very high temperature probe assembly.

# Bibliography

- [Correia] *Manufacture of backings for TOFD ultrasonic transducers*, Nilka ACEVEDO, Carlos CORREIA and Roberto OTERO, *Fundación Instituto de Ingeniería - Caracas*
- [Mrasek] *High Temperature Ultrasonic Transducers*, H. Mrasek, D. Gohlke, K. Matthies, E. Neumann, *Federal institute of Materials Research and Testing, Berlin*
- [Rubio] *Fabricación de Transductores Ultrasónicos para Equipos automatizados de inspección de líneas de Tuberías*, Carlos RUBIO, Obdulio MARRERO, *Centro de Ingeniería y Desarrollo Industrial (CIDESI); Querétaro, México (Spanish)*
- [Ju-Zhen] *US Patent 4800316, Jan, 24, 1989, Hu-Zhen*
- [Wang] *High Frequency Properties of Passive Materials for Ultrasonic Transducers*, Haifong Wang, Tim Ritter, Wenwu Cao and K. Kirk Shung, *IEEE*
- [Ruangsawad] *Characteristics of Al-epoxy Composite as Backing Material in Ultrasonic Transducer*, Anucha Ruangsawad<sup>1</sup>, Sirithan Jiemsirilers<sup>1</sup>, Pitak Lao-ratanakul, *1Research Unit of Advanced Ceramics, Department of Materials Science, Faculty of Science, Chulalongkorn University, Bangkok 10330, Thailand*
- [Grewe] *Acoustic Properties of Particle/Polymer Composites for Ultrasonic Transducer Backing Applications*, Martha G. Grewe, T. R. Gururaja, Thomas R Shroul and Robert E. Newnham
- [Applus Catalog] *Catalogue Ultrasonic Probes*, [www.ApplusRTD.com](http://www.ApplusRTD.com)
- [Gilardoni Catalog] *Catalogo ULTRASONIC PROBES*, [www.gilardoni.it](http://www.gilardoni.it)

## Chapter 4

# Piezoelectric Material Selection

**Industrial Production Process** The Figure 4.1, extracted from [8], summarize the production process of piezoceramics materials. Piezoceramic bulk elements are industrially manufactured from spray-dried granular material. The process to produce bulk disks starts with mixing of the raw materials (for a PZT:  $PbO$ ,  $TiO_2$ ,  $ZrO_2$  and various dopants). Next, the mixture is heated to 75 % of the sintering temperature to accelerate reaction of the components. The polycrystalline, calcinated powder is ball milled to increase its reactivity. Granulation with the binder is next to improve processing properties. After shaping and pressing the (green) ceramics is heated to 750 °C to burn out the binder. The next phase is sintering at temperatures between 1250 °C and 1350 °C. The sintered ceramic material is hard and can be sawn cut, ground, polished, lapped, etc., to the desired shape and tolerance if required. Screen printing is used to metallize the piezoelements and sputtering processes (Physical Vapour Deposition) are employed for thin silver layers. The sintered elements are then polarized. The last step is the poling process which takes place in a heated silicon oil bath at electrical fields up to several kV/mm.

### 4.1 Curie Temperature

As explained in [3] and [7] the temperature affect greatly the behavior of piezoelectric material. The Curie-Weiss temperature for a piezoelectric material is defined as the temperature at which the dielectric constant reach its maximum or, alternatively, the temperature above which the material loses its polarization and piezoelectric characteristics. As shown in [3], in PZT the piezoelectric  $d_{33}$  (that is the ratio between the strain and the electric field in direction  $i_3$  at zero stress) increase with the temperature, that is, oscillations of larger amplitude are required to record the same voltage output. Conversely, the coupling factor, that express the efficiency of the mechanical/electrical/mechanical energy conversion, will decrease.

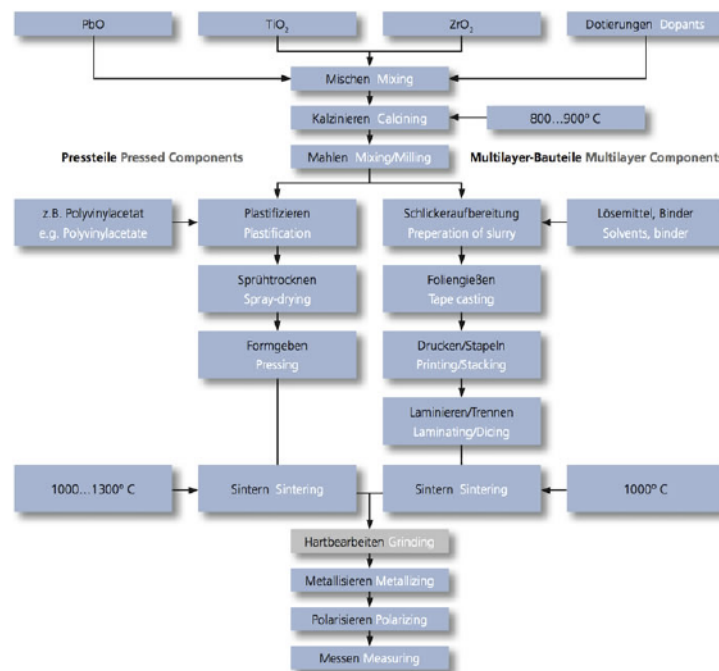


Table 4.1: Industrial manufacturing process of piezoceramics.

## 4.2 Qualitative Tests

As discussed in the thesis [4] and in the technical guide [5], for most piezoceramic materials, the maximum reasonable continuous operating temperature is about one-half of the Curie temperature, expressed in Celsius degrees.

In order to prototype an ultrasonic transducer capable of continuous operation at 250 °CNDEAA Lab has been provided with PZT5 piezoceramic disks. These disks are manufactured by APC International and their material code is 851. This material seemed to be very sensible even to the heat transmitted during soldering process. In Table 4.3 are shown impedance scannings covering the resonant frequency, before and after brazing a wire on the piezo without applying any strategy to contain the amount of heat transmitted.

The Curie Temperature reported in the datasheet of PZT5 851 is 360 °C. In order to compare qualitatively the effect of heat on different piezoelectric materials available at NDEAA Lab, 4 specimens have been selected for a test.

1. PZT5-851
2. PZT5-851 (already exposed to heat while brazing wires on its electrodes)
3. A common piezoelectric buzzer (Tapecast PZT5A)
4. PZT5H

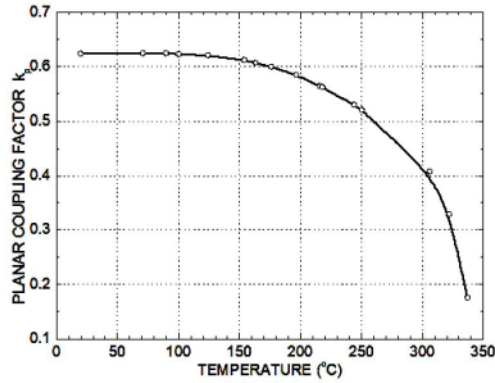


Table 4.2: From [3]. Temperature effect on coupling factor in "soft" PZT.

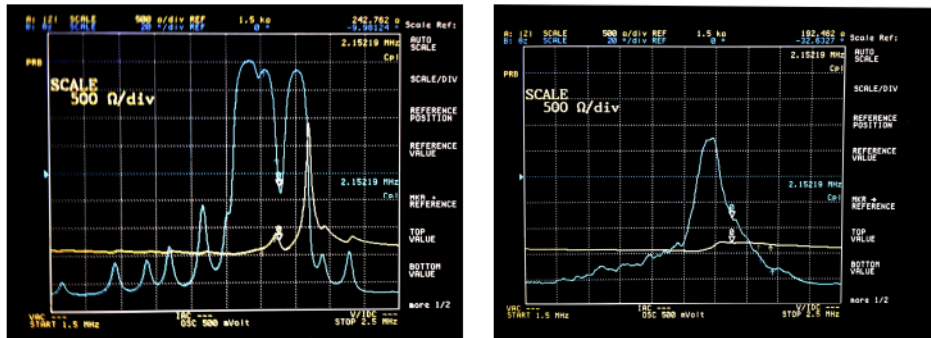


Table 4.3: Impedance Analysis of PZT5-851 from APC International (D = 10 mm h = 0.675 mm) Absolute value of complex impedance and phase. Before (left) and after rough soldering process.

Impedance scanning were performed at room temperature. A first scan was performed for each specimen, then all the piezos have been kept in the Blue M lab oven at a temperature of 250 °C for two hours. An impedance scanning was then repeated for each specimen. Table 4.4 shows the impedance scanning of the PZT5 851 before and after heat exposure. As it easy to see, the piezoelectric response is much weaker, proving that the piezo has been damaged. Table 4.5 shows that there is further degradation of the piezoelectric response also in the PZT5 that underwent a soldering operation. The impedance scanning of the buzzer exposed to heat is compared to a similar one. In this case, (Table 4.6) is not possible to asses any kind of change in the impedance spectrum. As shown in Table ??, the PZT5H lost completely it's piezoelectric behavior after heat exposure.

Since this analysis was only qualitative, wasn't possible to conclude that the PZT5-851 disks are not suitable for continuous operation at 250 °C. The more

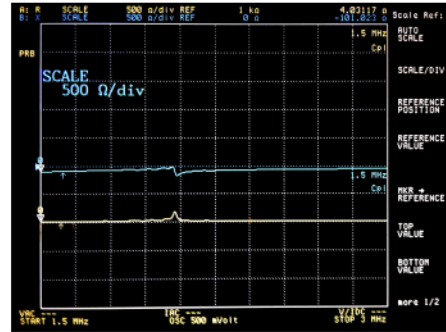
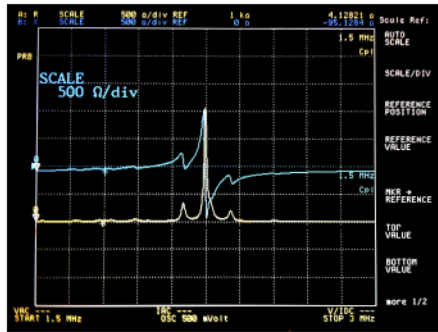


Table 4.4: Impedance Analysis of a PZT5 ( $D = 10$  mm,  $h = 0.675$  mm). Real and imaginary parts of complex impedance. Before (left) and after exposure to  $250$  °C for 2 hours.

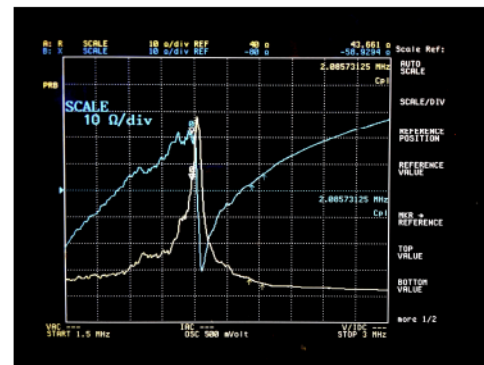
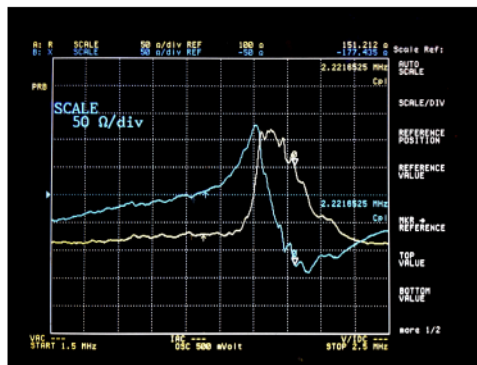
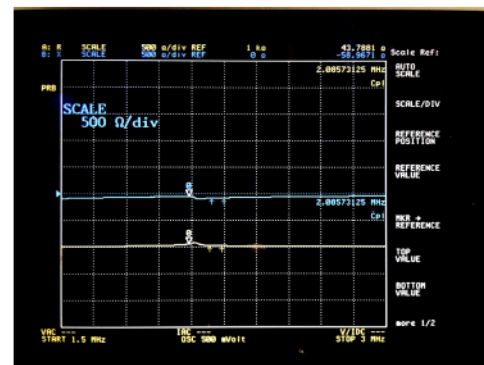
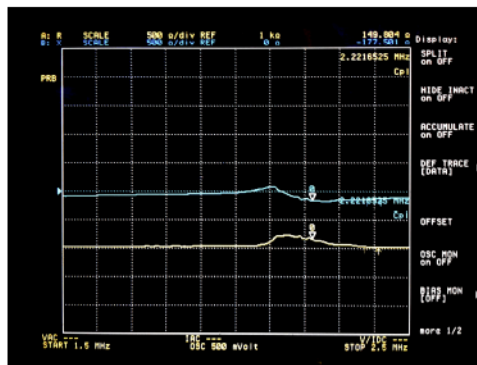


Table 4.5: Impedance Analysis of a PZT5-851 that underwent a rough soldering operation ( $D = 10$  mm,  $h = 0.675$  mm). Real and imaginary parts of complex impedance. Before (left) and after exposure to  $250$  °C for 2 hours.

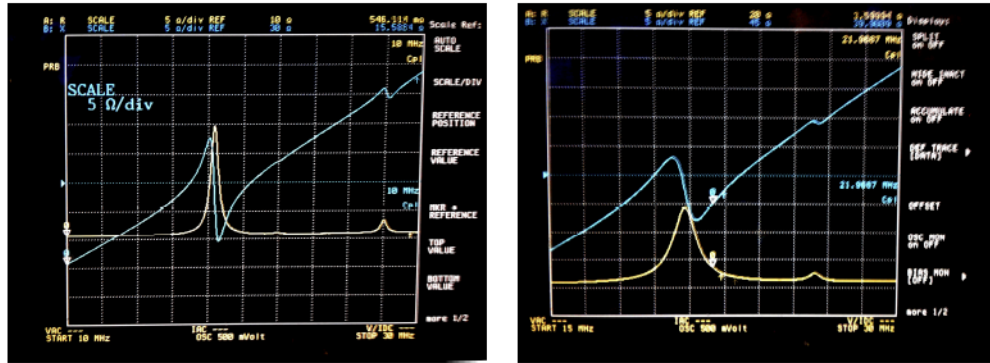


Table 4.6: Impedance Analysis of the Tape-cast PZT5A buzzer. Real and imaginary parts of complex impedance. Right: heat exposed specimen. Left: reference specimen.

complex equipment described in the previous chapters was then assembled and programmed to allow a more detailed tests.

### 4.3 Test of PZT5-851 piezoceramics

#### 4.3.1 In-Temperature Measurements

In order to quantify the performance parameters of the PZT5-851 disks at different temperatures, an in-temperature impedance scanning test was performed. The complex impedance was recorded at intervals of 5 minutes from 2 MHz to 2.5 MHz with a resolution of 2.5 KHz. The test was performed in the EC01 chamber raising the temperature in steps till 180 °C, cooling down to room temperature and then raising the temperature again to 250 °C. A Matlab script was written to mount all the data in a movie, as well as to calculate the planar coupling coefficient  $k_p$  and the  $h_{33}$  piezoelectric constant. The Figures 4.7, 4.8, 4.9, 4.10, 4.11 show the impedance scanning and the temperature recording respectively at the beginning of the test, when the specimen reached 180 °C, at the beginning of the second test after 12 hours, when the sample reached 210 °C, when the sample reached 250 °C.

The experimental setting is shown in Table 4.12. An accurate description of the devices has been already given in the past chapters.

#### 4.3.2 Quantitative Results

A Matlab script was developed to estimate the piezoelectric parameters  $h_{33}$  and  $k_t$ . This script uses a nonlinear regression technique to fit the data with a parametric model of the complex impedance as a function of the frequency  $f$ . As shown in [1] and [2] a model of the complex impedance  $Z$  for a free vibrating (unclamped) transducer is given by:

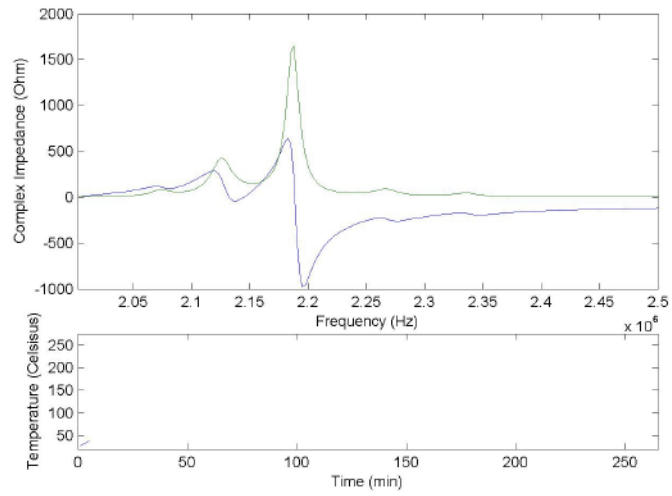


Table 4.7: Impedance scannings of PZT5-851 disk with  $D = 10$  mm and  $h = 0.675$  mm. Unsymmetrical clamping with about 0.1 kg, fixture-calibration of the impedance scanner not performed.

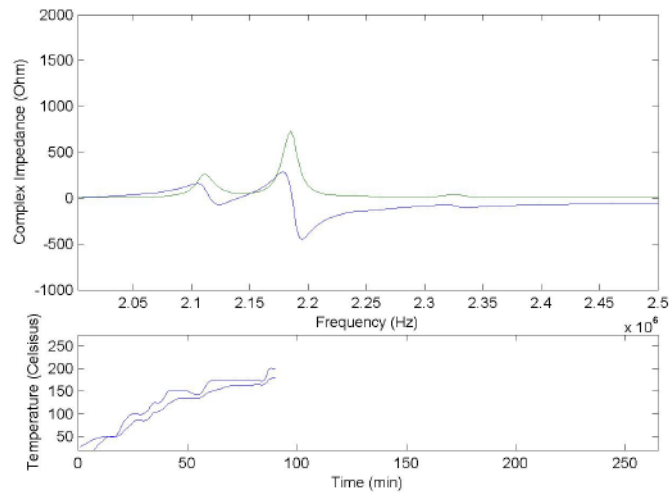


Table 4.8: Impedance scannings of PZT5-851 disk with  $D = 10$  mm and  $h = 0.675$  mm. Unsymmetrical clamping with about 0.1 kg, fixture-calibration of the impedance scanner not performed.

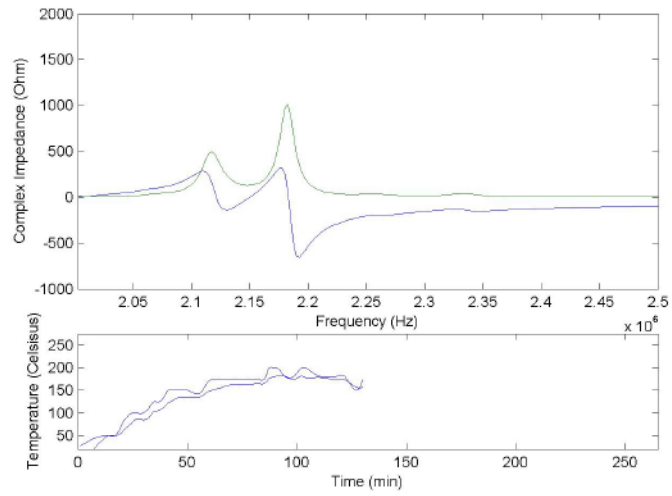


Table 4.9: Impedance scannings of PZT5-851 disk with  $D = 10$  mm and  $h = 0.675$  mm. Unsymmetrical clamping with about 0.1 kg, fixture-calibration of the impedance scanner not performed.

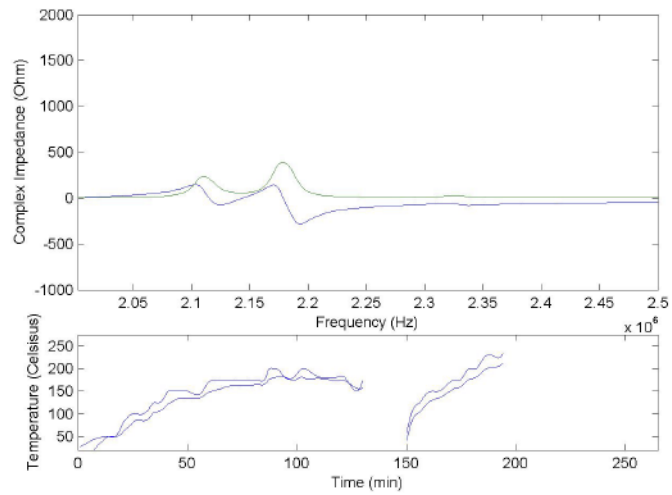


Table 4.10: Impedance scannings of PZT5-851 disk with  $D = 10$  mm and  $h = 0.675$  mm. Unsymmetrical clamping with about 0.1 kg, fixture-calibration of the impedance scanner not performed.

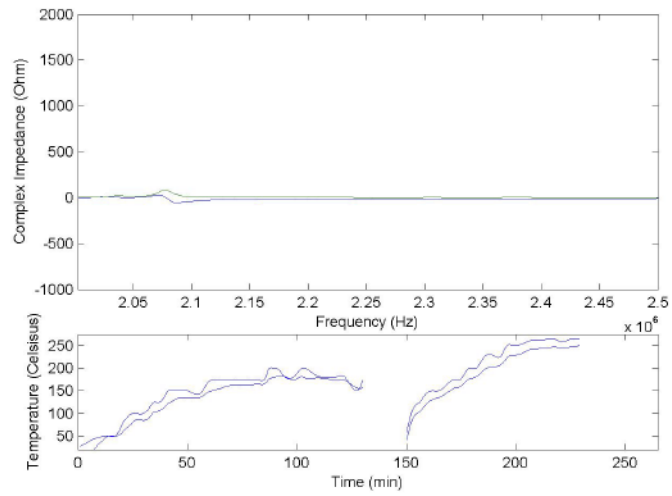


Table 4.11: Impedance scannings of PZT5-851 disk with  $D = 10$  mm and  $h = 0.675$  mm. Unsymmetrical clamping with about 0.1 kg, fixture-calibration of the impedance scanner not performed.



Table 4.12: Experimental setting for in-temperature impedance scanning tests.

$$\mathbf{Z}(f) = \frac{L}{i2\pi f \epsilon_{33}^S A} \left[ 1 - k_t^2 \frac{\tan\left(\pi f L \sqrt{\frac{\rho}{c_{33}^D}}\right)}{\pi f L \sqrt{\frac{\rho}{c_{33}^D}}} \right] \quad (4.1)$$

where  $\mathbf{Z}$ , the stiffness constant  $c_{33}^D$  and the  $\epsilon_{33}^S$  are complex parameter, while  $K_t$  is a real parameter. The other variables ( $L, A, \rho$ ), assumed to be constant, describe the geometry of the disk and its density.

The complex charge-stress piezoelectric constant  $\mathbf{h}_{33}$ , expressed in N/C or in V/m, could be computed following the definition of  $k_t$ :

$$\mathbf{h}_{33} = K_t \sqrt{\frac{c_{33}^D}{\epsilon_{33}^S}} \quad (4.2)$$

As described in the Matlab documentation, the function `nlinfit` perform a linear regression using the Gauss-Newton algorithm. A subset of data points around the resonant frequency was selected to run the algorithm and the coefficients taken from the datasheet were used as starting points of the iterations. The results of this approach are shown in the Table 4.14. The resulting trend is consistent with what described in [3], but the error of the algorithm is supposed to be relevant when the resonance peaks became barely detectable. The disappearing of the impedance peak, together with a strong decreasing trend of the piezoelectric coefficient, confirmed the depolarization of the specimen. A weak residual piezoelectric effect was noticed after cooling down.

#### 4.4 Test of TapeCast PZT5A Piezoceramics

This test involves a common and inexpensive piezoelectric buzzer made of PZT5A, manufactured with the tapecast technology. The experimental setting is the same of the previously described PZT5-851 test. This time the temperature was increased linearly using the `RATE=` command of the Environmental Chamber. The specimen temperature was recorded automatically using a termocouple. Figure 4.15 shows the impedance scanning at the beginning of the test, Figures 4.16 and 4.17 show the impedance at 250 °C and at 100 °C during cooling down. This test confirmed that PZT5A is suitable for high temperature use.

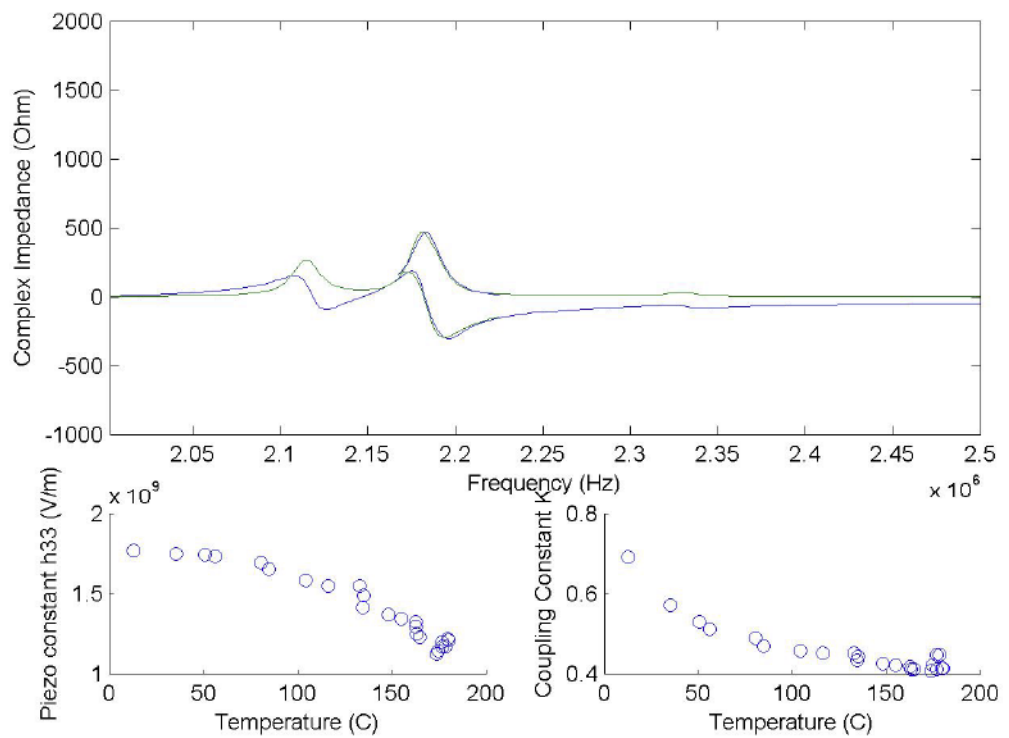


Table 4.13: Post processing of impedance scanings of PZT5-851 disk with  $D = 10$  mm and  $h = 0.675$  mm. Unsymmetrical clamping with about 0.1 kg, fixture-calibration of the impedance scanner not performed.

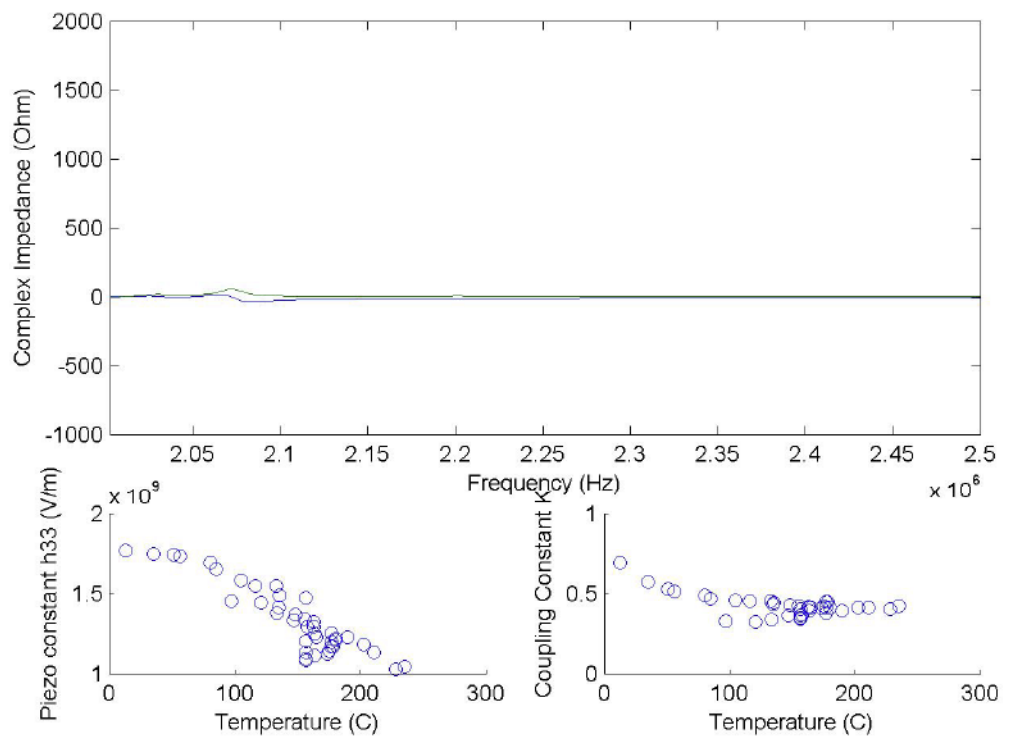


Table 4.14: Post processing of impedance scannings of PZT5-851 disk with  $D = 10$  mm and  $h = 0.675$  mm. Unsymmetrical clamping with about 0.1 kg, fixture-calibration of the impedance scanner not performed.

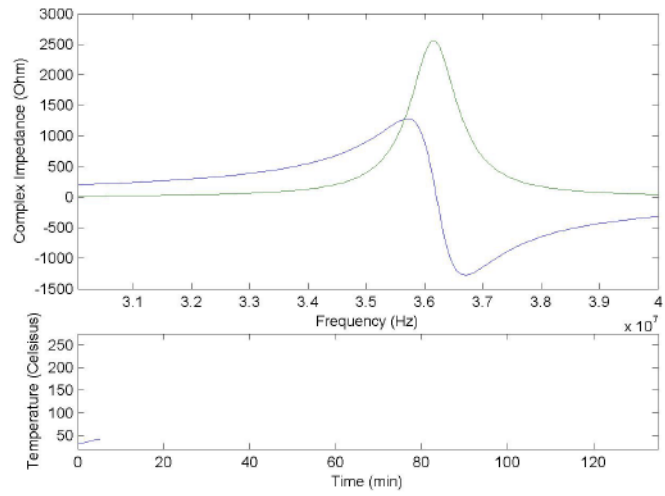


Table 4.15: Impedance scannings of PZT5A tapecast buzzer. Unsymmetrical clamping with about 0.1 kg.

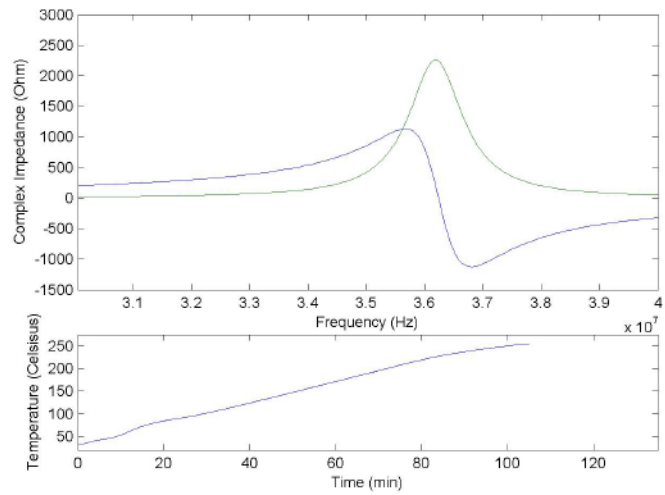


Table 4.16: Impedance scannings of PZT5A tapecast buzzer. Unsymmetrical clamping with about 0.1 kg.

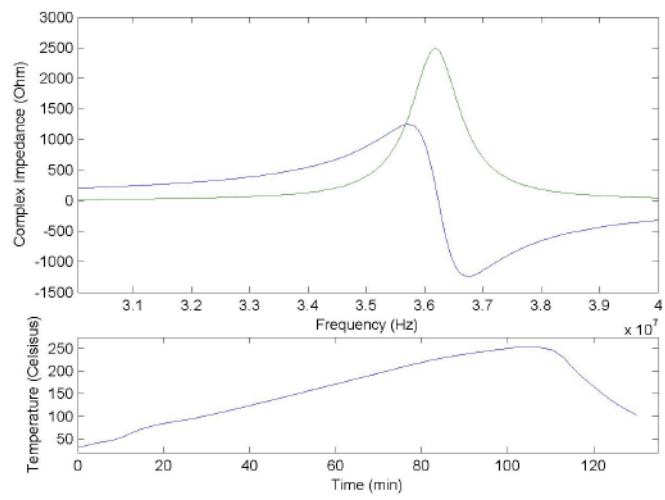


Table 4.17: Impedance scanings of PZT5A tapecast buzzer. Unsymmetrical clamping with about 0.1 kg.

# Bibliography

- [1] *Characterization of Piezoelectric Materials for Transducers*, Stewart Sherrit, Jet Propulsion Laboratory, Binu K. Mukherjee, Physics Department, Royal Military College of Canada
- [2] *Evaluation of the Material Parameters of Piezoelectric Materials by Various Methods*, Kin Wing Kwok, Helen Lai Wah Chan and Chung Loong Choy
- [3] *Effect of Temperature on The Main Piezoelectric Parameters of A Soft PZT Ceramic*, Miclea Et Al, *Romanian Journal of Information Science and Technology*
- [4] Hu, Wei, "Experimental search for high Curie temperature piezoelectric ceramics with combinatorial approaches" (2011). *Graduate Theses and Dissertations. Paper 10246*
- [5] *The piezoelectric effect in ceramic materials, Technical Guide*, <http://www.morganelectroceramics.com>
- [6] *PZT5 851 Datasheet*, <http://www.americanpiezo.com/apcmaterials/piezoelectric-properties.html>
- [7] *PI Piezotechnology Product Catalog and Technical Information*, [www.piezoceramic.com](http://www.piezoceramic.com)
- [8] *Piezo-ceramic Manufacturing Process*, CeramTech Technical Information, [www.ceramtech.com](http://www.ceramtech.com)

## Chapter 5

# Fabrication Technologies and Materials

### 5.1 Electrical Connection

#### 5.1.1 Electrodes

The faces of piezoelectric disks are usually screen-printed with silver pastes or sputtered with atomic silver. According to [1] and [3], the thickness of those layers range from 1 to 10  $\mu m$ . The adhesion strength of this layer is originally quite high (about 5 MPa for screen printed layers) but it became more weak after heat exposure, for example after a failed soldering attempt. Manufacturers of piezoelectric devices seems to be completely aware that soldering those silver electrodes could be challenging and that excessive heat could damage the ceramic as well as the electrode. Furthermore, as reported by [1] and [2], there can be problems with wetting the solder on the silver surface and soldering can then be difficult. This phenomenon is mainly caused by a reaction between sulphuric molecules in the atmosphere with the silver surface with the formation of a silver sulphide layer on the surface of the part. The formation and thickness of this layer is influenced by several factors such as age, pH, humidity, etc. In order to overcome this effect, manufacturers recommend to scratch gently the surface using a glass brush or a steel wool, but good results have been achieved also with sandpaper.

#### 5.1.2 Soldering

Manufacturers agree that the soldering time shouldn't exceed a couple of seconds. A flux paste is necessary to protect the electrode and the soldering material from oxidation during the process. As described in [2], a possible technique is to wet the wire with soldering material (tinning), than deposit a drop of flux paste on the electrode, immerse the tinned wire in that flux drop and then apply the tip of the soldering iron on top of the wire. An alternative technique is to let fall a drop of soldering material on the electrode, already wet with flux paste, position the

tinned wire and then apply the tip of the soldering iron to melt and let coalesce the soldering material. With this procedure was possible to obtain connections thick less than a millimeter. In order to fabricate connections that can stand 250 °C, an high temperature soldering material ( Multicore / Loctite - MM01006 ) with 93.5 % lead, 5 % tin and 1.5 % silver was selected. This material melts at about 300 °C, while common soldering materials with an almost eutectic ratio of lead and tin melt at 188 °C. Was noticed that even following a very strict procedure and keeping the iron tip in contact for less than a single second, the impedance scanning of PZT5-851 piezoceramics changed noticeably, denoting a local damage. Table 5.2 shows the impedance scanning before and after the soldering procedure performed at NDEEA lab with high melting point solder and a Weller WESD51 soldering station and basic electronic equipment.

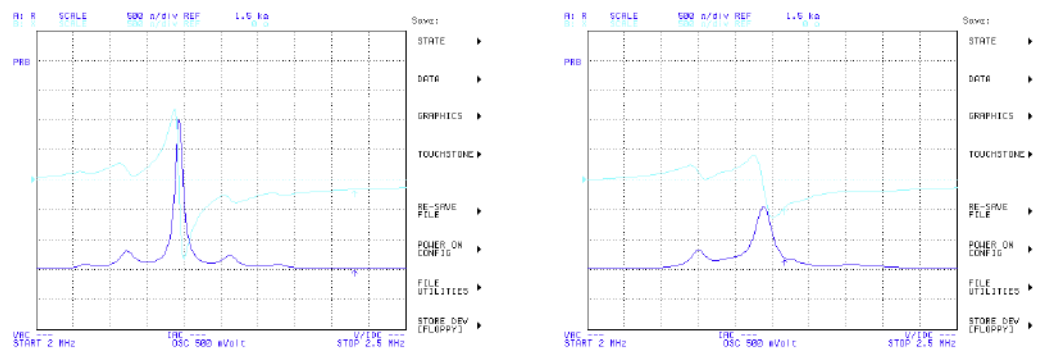


Table 5.1: Impedance scanning of PZT5-851 before and after soldering with traditional equipment.

In order to assess the sensitivity of the soldering process to the ability of the operator, soldering of two PZT5-851 was commissioned to the Electronic Assembly/Packaging Lab. The operation was performed by highly skilled technicians that reported how this unusual kind of soldering material is difficult to handle. The soldering was performed on an hotplate at 100 °C using the already mentioned high melting point soldering material and Alpha 615 Flux, using advanced equipment such as a binocular microscope and special manipulators. The soldering is more compact than the one obtained using traditional methods (less than a millimeter in thickness), but as shown in Figure 5.3, the resulting damage is comparable.

### 5.1.3 Silver Painting and Conductive Polymers

An alternative electrical connection technology was then investigated. Colloidal silver paint is a suspension of sub-micrometric silver flakes in iso-butyl methyl ketone. After evaporation on the alcohol, the silver flakes form a thin and smooth



Table 5.2: PZT5-851 soldered using basic electronic equipment, two PZR-851 soldered with advanced electronic equipment at Electronic Assembly/Packaging Lab.

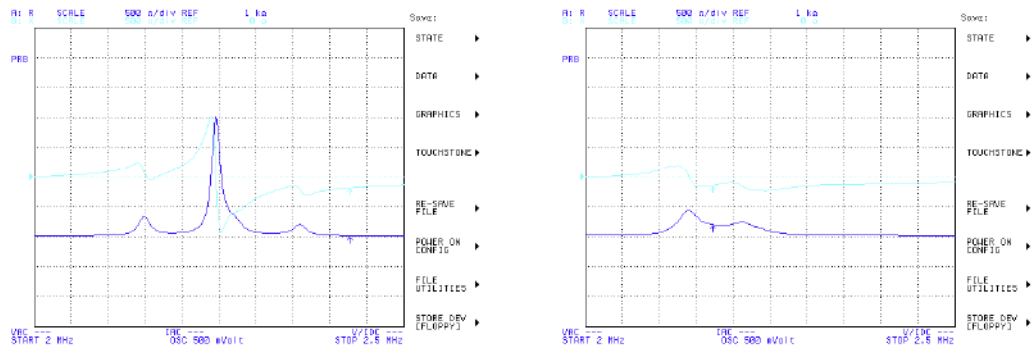


Table 5.3: Impedance scanning of PZT5-851 before and after soldering with advanced equipment at Electronic Assembly/Packaging Lab.

conductive film. This material is used to prepare specimens for scanning electron microscopy, but could be used also to repair the electrode of a piezoceramic or more generally to create electrical connections. Even if with colloidal silver is possible to wire a piezo without exposing it to heat, the silver layer was found to be to fragile.

The solution was found to be the gluing with silver filled polymeric material. That kind of materials, because of the need to have very accurate nanoparticles/polymer ratios, are generally available only in premixed form. For this reason, such materials have be kept at cryogenic temperatures to prevent the polymerization reaction to begin. The silver filled urethane tested seemed to be far more strong than the silver paint, but probably less conductive. The AiT MC8880 allows curing at temperatures in the range from 125 °C to 175 °C allowing electrical connection of temperature sensitives materials as well as fast bonding when there is no temperature limitation.

## 5.2 Polymer Molding

An aluminum mold with a very simple design was machined. In order to have ultrasonic waves with the same phase on the whole surface of the piezoelectric disk, the matching layer have to be of very constant thickness. To achieve this result, a very accurate positioning of the disk is required. The lower part of the mold was then fabricated with an indentation of 0.5 mm to hold the disk in position. A little chisel was also filed off to house the wire attached on the front side. The main problems was related to the resins sticking to the mold surfaces, even using many layers of mold release. Anoter proble was that the viscosity of most resins is quite high at room temperature, became extremely low when heated and start to increase again only when polymerization start taking place. For this reason, the fluid polymer could easily infiltrate between the different parts of the mold and flow away. This problem was addressed coating all the part of the mold with a spray mold release and then wetting the surface junctions with epoxy resin. A fast curing of the mold alone ensures a proper sealing of any gap. The same result could have been reached using room temperature glues or building a mold with extremely tight mechanical tolerances. Table 5.4 shows a cylindrical aluminum mold with with a diameter of 14 mm.



Table 5.4: Impedance scanning of PZT5-851 before and after soldering with advanced equipment at Electronic Assembly/Packaging Lab.

# Bibliography

- [1] *Piezoelectric Electrodes: Soldering to Silver Electrodes. Morgan Technical Ceramics, <http://www.morganelectroceramics.com>*
- [2] *Soldering Instructions, Boston Piezo-Optics Inc., [www.bostonpiezooptics.com](http://www.bostonpiezooptics.com)*
- [3] *PI Piezotechnology Product Catalog and Technical Information, [www.piezoceramic.com](http://www.piezoceramic.com)*
- [4] *Piezoelectric Sound Components, Application Manual, Murata Manufacturing Co., Ltd.*

## Chapter 6

# In-House Built Prototypes

### 6.1 Early prototypes

A first prototype was built to test the damping proprieties of the SOLITHANE 113 urethane resin. The resin was retrieved premixed with a curing agent and a plasticiziser. This premixed form has to be stored at the temperature of  $-80\text{ }^{\circ}\text{C}$  and, as instructed by the technicians of the Polymerics Application Laboratory, has a pot life of less than half an hour. The refrigerator available at NDEEA lab is not capable of reaching the required temperature of  $-80\text{ }^{\circ}\text{C}$ , then is not suitable for a long term storage of the polymer. Storage in a common refrigerator (temperature of about  $-20\text{ }^{\circ}\text{C}$ ), even for a few hours, is strongly unrecommended. A TRS Ceramics PZT4 Piezoelectric crystal with a diameter of 12 mm and an height of 4 mm was used. The resonant frequency of this transducer is about 500 KHz. This piezoelectric material is not suitable for high temperature testing, for this reason common wires were used. The waveform produced by a pulse-echo test is shown in Figure 6.1. As reported by the datasheet, the elastic modulus of the polymer is less than 4 MPa. The speed of sound in a material is

$$v = \sqrt{\frac{E}{\rho}} \quad (6.1)$$

then the acoustic impedance will be  $\sqrt{\rho E}$ . The acoustic impedance of this polymer will be then very different from the one of steel. Since this polymer was expected to become even more soft at high temperatures, this polymeric material was discarded. As expected, the damping of the first pulse was also insufficient. The transducer was tested on a 10 cm aluminum block and produced the signal shown in Table 6.1. As it's possible to see, the first echo is almost completely covered by the noise. The amplitude of the second signal is about two time the average noise between 50 and 100 microseconds. The matching layer, thick less than a millimeter, proved to have a too low acoustical impedance to transmit properly the signal.

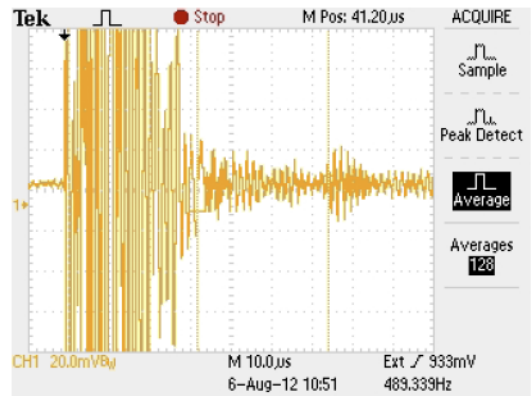
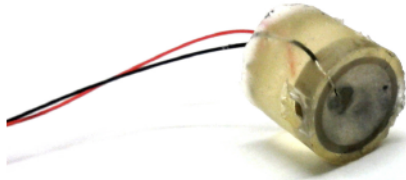


Table 6.1: A first in-house built prototype of ultrasonic transducer and the echo-pulse reading over a 10 cm aluminum block.

Another prototype was built using a two part epoxy for aerospace bonding purposes, the Hysol EA 9361, and a 2 mm PZT4 piezoelectric disk with a resonant frequency of 1.200 MHz. A similar behavior was observed: the damping of the first pulse was insufficient. Figure 6.2 shows the signal postprocessed with a bandpass filter.

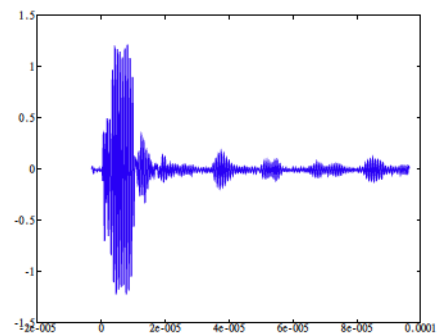
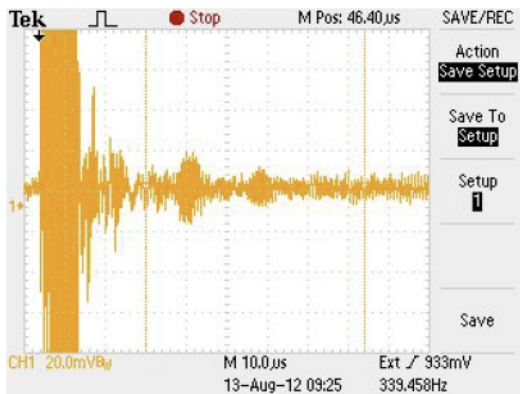


Table 6.2: Signal recorded from the second in-house built prototype of ultrasonic transducer when tested over a 10 cm aluminum block. Effect of the application of a band-pass filter to the signal.

## 6.2 Prototypes

### 6.2.1 Polymeric multilayer transducer

To reduce the noise and allow the detection of an even more weak echo, a multilayer transducer was built. The fabrication was made in multiple steps and because of its complexity was successful only at the third attempt. The whole process could be summarized as follows:

**Wires connection.** The wires were hammered to reduce their thickness and then attached using a very little amount of silver filled urethane MC8880 from AiT. The curing of the disk and the wires was performed at 125 °C for 2 hours following the instruction of the datasheet. Heat tolerant piezoceramics allows to cure at higher temperatures for shorter times.

**Mold sealing.** The mold was assembled and sealed using the procedure described in the previous chapter. A new design of the mold or more strict dimensional tolerances could allow to skip this step.

**Positioning of the piezoceramic** The transducer was put in the mold and carefully positioned in order to have its faces perpendicular to the mold axis. The front face of the piezo was at less than a millimeter to the bottom end of the mold. In the only successful molding, positioning was achieved holding the piezo by both of its wires using a common third hand (holder for electronic operations). An alternative approach to have a better angular tolerance could be to stick a rod on the back of the piezo using a very weak glue and then use a dedicated support to hold the rod aligned with the mold.

**Molding of the matching layer.** Some drops of Duralco 4460 resin was poured in the mold. An extremely thin layer of resin filled completely the space between the front of the ceramic and the bottom end of the mold. Much attention was paid to not wet the back layer of the piezoceramic disk. The curing at 120 °C for 4 hours polymerized the front layer.

**Molding of the backing layer.** About 1 cc of a mixture of tungsten powder ( 10% in volume ) and MC7880 urethane resin from AiT was poured on top of the piezo. Curing at 125 °C for 30 minutes polymerized the backing layer

**Final molding** In order to have a transducer easier to handle, the mold was topped up with about other 3 cc of Duralco 4460 resin. Curing was again at 120 °C for 4 hours. In the future, this step could be used to bond a metallic attachment or an electrical connector just immersing it into the polymer.

**Opening of the mold.** The transducer was carefully extracted from the aluminum mold.

This multilayer transducer is shown in Table 6.3. As expected, the tungsten/urethane backing succeed in damping the pulses in a very short time. The transducer produced results inferior to commercial transducers while tested on the aluminum block but was able to detect the oil-air interface when put on the back of the half-pipe testbed. The required pressure was particularly high and had to be applied in a very asymmetric way to obtain a good signal. Field usage of this prototype is therefore completely unpractical, considering that the piezoelectric material is not capable of working at high temperature. Table 6.3 shows both the transducer and the very weak signal that was possible to gather.

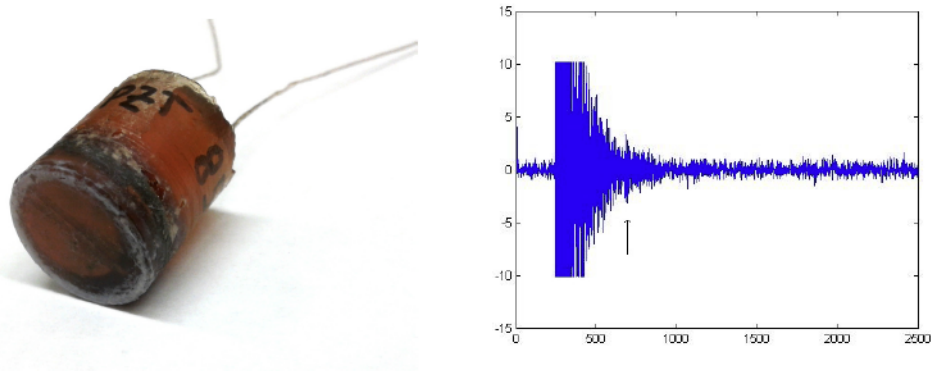


Table 6.3: A multilayer piezoelectric transducer. Signal when tested over the half-pipe testbed. The arrow point to the echo reflected from the oil-air interface.

### 6.2.2 No matching layer / bulk brass backing

Another design was explored to test the performance of a metallic backing. This prototype, shown in Table was built without connecting anything to the front layer. The front electrode, touching the alluminum block, was electrically connected to it during test. For this reason, the ground cable was attached directly to the aluminum block, while the signal cable was linked to the rear electrode using conductive epoxy. The piezoelectric disk was made of Lead Zirconium Titanate (EC-64) and manufactured by EDO Ceramics. The brass was chiseled to house the bulk wire attachment, and the piezoelectric disk was attached to the brass backing using a little amount of Duralco 4460 epoxy. The transducer and a the resulting waveform obtained during the usual test on the aluminum block are shown in Table 6.4. As it's possible to see, the signal has a very high amplitude. This result underline that most of the issues encountered in building an ultrasonic transducer are related to the matching layer. The absence of a real matching layer, with the sputtered silver electrode touching directly the object under test, resulted in echoes of great amplitude.

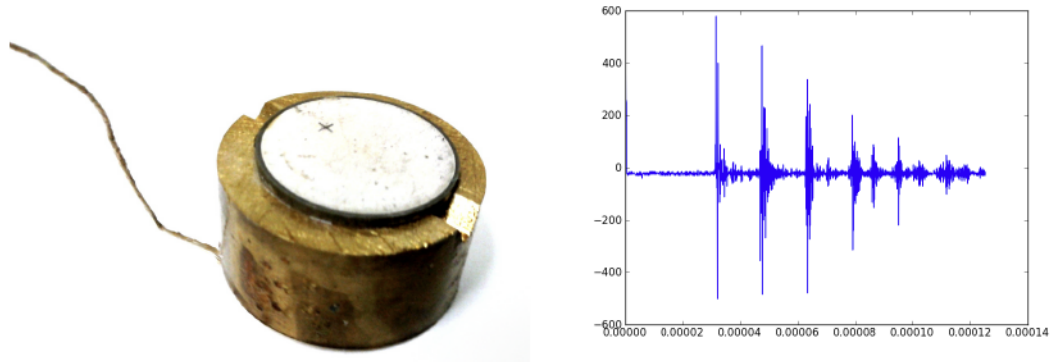


Table 6.4: A multilayer piezoelectric transducer. Signal when tested over the half-pipe testbed.

### 6.2.3 Thin copper-copper assembly

In order to observe the behavior of a transducer without a backing, that is, irradiating in free air on the rear side, an extremely simple prototype was built (Figure 6.5). Copper foils were scratched gently with sand paper to improve the adhesion strength and attached to a PZT5-851 disk using the silver filled urethane MC8880 from AiT. The disk has a thickness of 1 mm, a diameter of 10 mm and a resonance frequency of about 2 MHz. Curing was performed at 125 °C in order prevent the piezoelectric from damaging. The only challenging part of this process was to make sure that the silver filled urethane didn't crate any contact between the electrodes. A measurement with an electrical tester confirmed that there was no electrical connection (shorting) between the electrodes. The transducer was tested on the usual 5 cm aluminum block. In this prototype the front copper foil act both as a matching layer and as an electrode. Results are shown in Table 6.5. It's possible to see that the obtained signal is quite sharp. Was also noticed that pressing the transducer against the object being sensed with a metallic tool or with a finger change drastically the noise level. This observation suggest the possibility of using such a simple transducer to test a great variety of backing materials just pressing them on the rear copper electrode.

This transducer was the only able to measure clearly the thickness of the 5 cm aluminum block using both the 20 dB and the 40 dB voltage gain provided by the pulser/amplifier, that is, was the only able to work with large and small signals. Table 6.6 shows this achievement. This transducer was also able to detect the oil level in the half pipe testbed. As shown in Table 6.7, the quality of the signal is comparable to what obtained with commercial products. In order to ensure that the echo effectively comes from the oil-air interface, a small basin was immersed upside-down, keeping some air inside and was used to move the oil-air surface up and down. The shift of the echo accordingly to the oil-surface position



Table 6.5: Copper matching layer/no backing transducer.

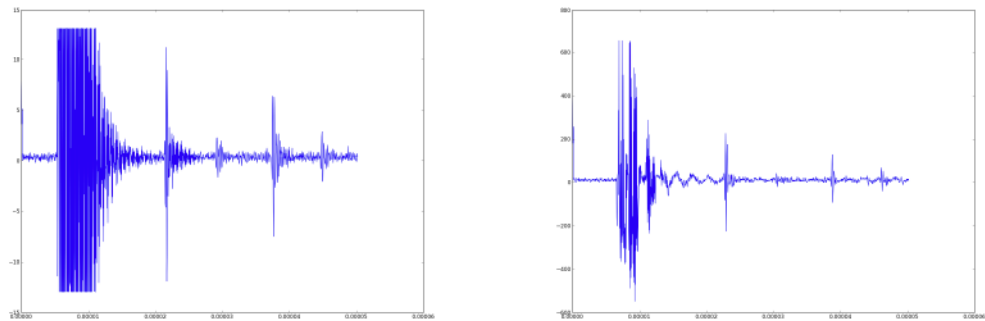


Table 6.6: Signal from the copper matching layer/no backing transducer when tested over the aluminum block. Voltage amplification was set to 20dB (left) and 40dB (right).

definitively confirmed this result. The quality of the signal was noticed to be extremely dependent to the quality of the mechanical contact of the transducer with the steel pipe as well as to the smoothness of the oil-air interface. An unsteady surface, caused for example by a fast movement of an object immersed in the oil, make the signal more faint. Even if this transducer was by far the most simple to build, its performances overcome the ones of all the other prototypes.

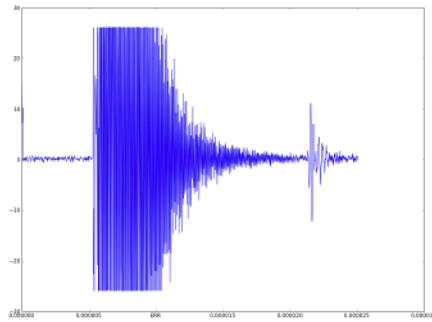


Table 6.7: Signal from the copper matching layer/no backing transducer when positioned on the back of the half pipe testbed.

# Bibliography

- [1] *Solithane 113 Datasheet, Compton Chemical*
- [2] *Hysol EA 9361 datasheet, Henkel COrporation Aerospace Group*
- [3] *MC8880 Datasheet, AiTechnologies Inc.*
- [4] *MC7880 Datasheet, AiTechnologies Inc.*
- [5] *Duralco 4460 Cotronics Corp.*

# Chapter 7

## Summary

This chapter will summarize the conclusions of the present work, discuss which are the current issues and difficulties and discuss some proposal to address those .

### 7.1 Conclusions

**The best results were obtained from an extremely simple transducer** Transducers with a metallic matching layer seems to perform better than transducer with a polymeric matching layer and a polymeric backing.

**PZT5-851 and PZT4 are not suitable to high temperature use** Coherently with the datasheet provided by APC International, was shown that PZT5-851 is not suitable for high temperature use.

**Silver filled urethane is a very effective material to make electrical connection**

The usage of this composite to connect termosensitive material is common among material scientists working on piezoelectric materials. This technique allows also to create connection more flat than soldering.

**The urethane resin Solithane 113 is not stiff enough to build transducers**

The elastic modulus of this polymer at room temperature is less than 4 MPa. The acoustic impedance is the just two time the impedance of the water and it's not enough to couple ceramic and steel.

**The tungsten filled urethane is effective in damping vibrations**

The characteristic damping time of the pulse in a piezoelectric disk (PZT5-851) diminish more when embedded in a transducer with a tungsten filled urethane backing than when embedded in transducer made only of epoxy.

## 7.2 Issues and open problems with proposed solutions

**The depolarization wasn't quantified except for a single case** In the previous chapters were shown the results of the computation of the piezoelectric coefficients using nonlinear regression (Gauss-newton algorithm) over the impedance spectrum. Even if the decreasing trend was clearly identified, wasn't possible to calculate the exact coefficients. The algorithm currently in use takes into account only the complex impedance, while it's immediate to show that little deviations from the complex impedance  $Z = R + jX$  could result in large deviations from the complex admittance  $Y = Z^{-1} = G + jB$ . The algorithm should then be rewritten to optimize the fit both on  $Z$  and on  $Y$ .

**It's difficult to position the piezoelectric crystal in the mold** It's very important to have a matching layer of the same thickness on the whole surface of the disk. A possible solution to have the crystal perpendicular to the axis is to stick the crystal to a metallic rod, that is easier to take in place, using a weak glue. (See chapter 6 for more details about the fabrication process)

**The recorded data are sensible to the settings of the Pulser/Amplifier** It's quite difficult to compare different transducer tested in different times. The LabView program could be updated again to take into account each particular setting of the Oscilloscope. Since the Pulse/Amplifier is an analog device, is not possible to do the same and the settings have to be recorded manually or photographed. A new programmable Pulser/Amplifier would allow to record those settings automatically and also change them dynamically while the temperature increase to fit the new electromechanical proprieties of the transducer.

**The silicon oil change its acoustic proprieties over a wide range** Was observed that the speed of sound in silicon oil at 250 °C is about one half of the speed at room temperature. This problem have to be addressed interpolating wit a polinomial the speed of sound as a function of the temperature. Thermal expansion and the geometry of the pipe will have to be taken into account.

**Most materials have been tested only before and after heat exposure** Since the the software interface is already in place, will be possible to make tests in an highly automated way, taking measurement in a wide range of temperatures.

**The couplant fluid currently in use withstand oxidation reaction** The couplant fluid currently in use, even if rated for temperature till 350 °C, burn after some minutes at 250 °C, leaving nothing more than a crust that doesn't

allow mechanical coupling. Many tests produced wrong results from a certain point on because of this phenomena. A different couplant fluid should be identified.

enddescription

#### ACKNOWLEDGEMENT

This report describes research and development work that was conducted at the Jet Propulsion Laboratory (JPL), California Institute of Technology, and was sponsored by JPL's Visiting Student Research Program (JVS RP), under a contract with the National Aeronautics and Space Administration (NASA).

# Bibliography

- [1] *Piezoelectric Electrodes: Soldering to Silver Electrodes. Morgan Technical Ceramics, <http://www.morganelectroceramics.com>*